



THE UNIVERSITY *of* EDINBURGH

Edinburgh Research Explorer

## A divide-and-conquer approach for genomic prediction in rubber tree using machine learning

**Citation for published version:**

Aono, AH, Francisco, FR, Souza, LM, Gonçalves, PDS, Scaloppi, EJ, Guen, VL, Fritsche-Neto, R, Gorjanc, G, Quiles, MG & de Souza, AP 2022 'A divide-and-conquer approach for genomic prediction in rubber tree using machine learning' bioRxiv, bioRxiv. <https://doi.org/10.1101/2022.03.30.486381>

**Digital Object Identifier (DOI):**

[10.1101/2022.03.30.486381](https://doi.org/10.1101/2022.03.30.486381)

**Link:**

[Link to publication record in Edinburgh Research Explorer](#)

**Document Version:**

Publisher's PDF, also known as Version of record

**General rights**

Copyright for the publications made accessible via the Edinburgh Research Explorer is retained by the author(s) and / or other copyright owners and it is a condition of accessing these publications that users recognise and abide by the legal requirements associated with these rights.

**Take down policy**

The University of Edinburgh has made every reasonable effort to ensure that Edinburgh Research Explorer content complies with UK legislation. If you believe that the public display of this file breaches copyright please contact [openaccess@ed.ac.uk](mailto:openaccess@ed.ac.uk) providing details, and we will remove access to the work immediately and investigate your claim.



# A divide-and-conquer approach for genomic prediction in rubber tree using machine learning

Alexandre Hild Aono<sup>a,b</sup>, Felipe Roberto Francisco<sup>a</sup>, Livia Moura Souza<sup>a,c</sup>, Paulo de Souza Gonçalves<sup>d</sup>, Erivaldo J. Scaloppi Junior<sup>d</sup>, Vincent Le Guen<sup>e,f</sup>, Roberto Fritsche-Neto<sup>g</sup>, Gregor Gorjanc<sup>b</sup>, Marcos Gonçalves Quiles<sup>h</sup>, Anete Pereira de Souza<sup>a,i,\*</sup>

<sup>a</sup> *Molecular Biology and Genetic Engineering Center (CBMEG), University of Campinas (UNICAMP), Campinas, Brazil*

<sup>b</sup> *The Roslin Institute, The University of Edinburgh, Midlothian, United Kingdom (UK)*

<sup>c</sup> *São Francisco University (USF), Itatiba, Brazil*

<sup>d</sup> *Center of Rubber Tree and Agroforestry Systems, Agronomic Institute (IAC), Votuporanga, Brazil*

<sup>e</sup> *Centre de Coopération Internationale en Recherche Agronomique pour le Développement (CIRAD), UMR AGAP, F-34398, Montpellier, France*

<sup>f</sup> *AGAP, Univ Montpellier, CIRAD, INRAE, Institut Agro, Montpellier, France*

<sup>g</sup> *Departamento de Genética, Escola Superior de Agricultura “Luiz de Queiroz” (ESALQ), Universidade de São Paulo (USP), Piracicaba, Brazil*

<sup>h</sup> *Instituto de Ciência e Tecnologia, Universidade Federal de São Paulo (UNIFESP), São José dos Campos, Brazil*

<sup>i</sup> *Department of Plant Biology, Biology Institute, University of Campinas (UNICAMP), Campinas, Brazil*

---

\*Corresponding author

*Email addresses:* alexandre.aono@gmail.com (Alexandre Hild Aono), felipe.roberto.francisco@gmail.com (Felipe Roberto Francisco), liviamoura31@gmail.com (Livia Moura Souza), paulog@iac.sp.gov.br (Paulo de Souza Gonçalves), scaloppijr@yahoo.com.br (Erivaldo J. Scaloppi Junior), vincent.le\_guen@cirad.fr (Vincent Le Guen), roberto.neto@usp.br (Roberto Fritsche-Neto), gregor.gorjanc@roslin.ed.ac.uk (Gregor Gorjanc), quiles@unifesp.br (Marcos Gonçalves Quiles), anete@unicamp.br (Anete Pereira de Souza)

## Abstract

Rubber tree (*Hevea brasiliensis*) is the main feedstock for commercial rubber; however, its long vegetative cycle has hindered the development of more productive varieties via breeding programs. With the availability of *H. brasiliensis* genomic data, several linkage maps with associated quantitative trait loci (QTLs) have been constructed and suggested as a tool for marker-assisted selection (MAS). Nonetheless, novel genomic strategies are still needed, and genomic selection (GS) may facilitate rubber tree breeding programs aimed at reducing the required cycles for performance assessment. Even though such a methodology has already been shown to be a promising tool for rubber tree breeding, increased model predictive capabilities and practical application are still needed. Here, we developed a novel machine learning-based approach for predicting rubber tree stem circumference based on molecular markers. Through a divide-and-conquer strategy, we propose a neural network prediction system with two stages: (1) subpopulation prediction and (2) phenotype estimation. This approach yielded higher accuracies than traditional statistical models in a single-environment scenario. By delivering large accuracy improvements, our methodology represents a powerful tool for use in *Hevea* GS strategies. Therefore, the incorporation of machine learning techniques into rubber tree GS represents an opportunity to build more robust models and optimize *Hevea* breeding programs.

*Keywords:* deep learning, genomic selection, *Hevea brasiliensis*, neural networks, rubber tree growth.

## 1. Introduction

Rubber tree (*Hevea brasiliensis*) has an elevated importance in the global economy, being almost the only feedstock for commercial rubber (Cros et al., 2019; Warren-Thomas et al., 2015). Considering the long perennial vegetative cycle of *Hevea*, breeding programs aim to improve its yield production in order to reach the rapidly increasing rubber demand (Ahrends et al., 2015; Cros et al., 2019; Warren-Thomas et al., 2015). Therefore, genomic approaches are needed in rubber tree breeding, especially considering its recent domestication history (Rosa et al., 2018). *H. brasiliensis* is a diploid species ( $2n = 36$ ) with an elevated occurrence of duplicated regions in its genome ( $\sim 70\%$ ) (Lau et al., 2016; Liu et al., 2020; Tang et al., 2016), and this complex genomic organization has hindered the development of genomic strategies for breeding. However, with the improvement of next-generation sequencing (NGS) technologies and the consequent reduction in genotyping costs, data generation has become more efficient, providing more genomic resources in less time and with lower associated costs (Roorkiwal et al., 2018). This greater availability of data improved precision in selection with higher genetic gains in various crops (González-Camacho et al., 2018; Roorkiwal et al., 2018) and, in rubber tree, could complement traditional approaches based on only phenotypic and pedigree information (Hayes et al., 2013; Roorkiwal et al., 2018).

Various rubber tree genomic resources have become available in recent decades, such as a large set of different molecular markers (Lespinasse et al., 2000b; Nakkanong et al., 2008; de Souza et al., 2016; Venkatachalam et al., 2006), draft genomes (Lau et al., 2016; Tang et al., 2016), and, more recently, a chromosome-level assembled genome (Liu et al., 2020). These data have already allowed the construction of saturated linkage maps with associated quantitative trait loci (QTLs), which were proposed as a tool for marker-assisted selection (MAS) (An et al., 2019). Although QTLs for several traits have been identified in rubber tree (An et al., 2019; Le Guen et al., 2011, 2007; Lespinasse et al., 2000a; Rosa et al., 2018; Souza et al., 2013; Tran et al., 2016), the amount of phenotypic variance explained by these identified QTLs is usually small (Souza et al., 2013) because of the highly complex genetic architectures associated with growth and rubber production traits. The configuration of these phenotypes is controlled by many genes with small effects (Washburn et al., 2019), and weak QTLs may

30 not be identified using existing methodologies (Cros et al., 2019; Muranty et al., 2015), which  
31 prevents the identification of interindividual differences (Bellot et al., 2018). Together with  
32 the environmental and genetic background restrictions of QTLs (Crossa et al., 2017), these  
33 features limit the application of *Hevea* QTLs for MAS (de Souza et al., 2016). Consequently,  
34 novel genomic strategies that can assist in rubber tree breeding programs are needed, especially  
35 considering the time required to evaluate these phenotypes, the elevated costs, and the low  
36 female fertility in *H. brasiliensis* (An et al., 2019; Cros et al., 2019; Souza et al., 2019).

37 Aimed at solving such difficulties in many crops, genomic selection (GS) has arisen as  
38 a promising methodology for considerably reducing the required breeding cycle (Hayes et al.,  
39 2001). GS has shown better performance than MAS (Bernardo & Yu, 2007; Heffner et al., 2010),  
40 mainly because of its associated genetic gains (Albrecht et al., 2011) and reduced costs over a  
41 long time period (Wang et al., 2018). This strategy enables the selection of plants based on their  
42 estimated performance obtained with a large dataset of molecular markers (Ma et al., 2018;  
43 Roorkiwal et al., 2018), reducing breeding time by avoiding the need to evaluate a considerable  
44 number of phenotypes over different years (Crossa et al., 2017). Using known phenotypic and  
45 genotypic information from a training population (Crossa et al., 2019), it is possible to create a  
46 predictive model that can be used to predict the breeding values of a testing population using  
47 only genotypic data (Roorkiwal et al., 2018). This modeling is generally based on a mixed-  
48 effect regression method (Montesinos-López et al., 2018) and has already been demonstrated  
49 to be promising for several crops (Crossa et al., 2016; Spindel et al., 2015; Wolfe et al., 2017;  
50 Xavier et al., 2016; Zhao et al., 2012). In rubber tree, Souza et al. (2019) and Cros et al. (2019)  
51 assessed the potential of GS for predicting stem circumference (SC) and rubber production  
52 (RP), respectively, simulating breeding schemes through cross-validation (CV) techniques.

53 There are several CV approaches for simulating a real application of GS in a plant breeding  
54 program. These methods take into account the population structure in the dataset and the  
55 appropriateness of applying the developed predictive model to a set of plants. There are  
56 basically three approaches, which are used to (1) predict traits in an untested environment  
57 using previously tested lines (CV0) (Roorkiwal et al., 2018), (2) predict new lines' traits that  
58 were not evaluated in any environment (CV1) (Montesinos-López et al., 2019b), and (3) predict

59 traits that were evaluated in some environments but not in others (CV2) (Jarquín et al., 2017).  
60 These three scenarios were already evaluated in rubber tree. Cros et al. (2019) assessed the  
61 potential of GS in a within-family context using CV0 and CV1 methods, and Souza et al.  
62 (2019) tested three different populations with CV1 and CV2. These initiatives represent the  
63 first attempts to use GS on rubber tree data, but with low associated predictive capabilities  
64 for some of the created CV schemes, mostly when prediction is performed with genotypes that  
65 have not already been tested.

66 Different approaches have been used in GS to create predictive models, including parametric  
67 and nonparametric methods (Crossa et al., 2017; De Los Campos et al., 2009; Endelman, 2011;  
68 Hayes et al., 2001; Jannink et al., 2010; VanRaden, 2007, 2008). Significant differences in  
69 predictive capabilities have not been demonstrated when changing the predictive approach (Ma  
70 et al., 2018; Roorkiwal et al., 2016; Varshney, 2016); thus, linking genotypes and phenotypes  
71 remains a great challenge (Bellot et al., 2018; Harfouche et al., 2019), especially for plant species  
72 with high genomic complexity. In this context, more robust techniques for estimating these  
73 models with higher prediction capabilities are needed to expand the practical implementation  
74 of GS in rubber tree. Nonlinear techniques have already shown improved performance in  
75 representing complex traits with nonadditive effects (Crossa et al., 2014; González-Camacho  
76 et al., 2012, 2018; Pérez-Rodríguez et al., 2012), and, in this context, machine learning (ML)  
77 strategies have emerged as a promising set of tools for complementing these statistical nonlinear  
78 methods.

79 The objective of this work was to develop a genomic prediction approach for rubber tree  
80 data. Considering that ML methods have not been proven to have better performance than sta-  
81 tistical methodologies for GS (Bellot et al., 2018; Montesinos-López et al., 2019a), we evaluated  
82 their efficiency in rubber tree, also suggesting a novel approach for constructing a predictive sys-  
83 tem with neural networks based on two-stage prediction: (1) subpopulation prediction and (2)  
84 phenotype estimation. Such a divisive approach was created considering a common paradigm in  
85 Computer Science: divide and conquer. For datasets with a clear subpopulation structure, such  
86 as rubber tree, the proposed approach represents a promising alternative for the development  
87 of predictive models.

## 88 **2. Material and methods**

### 89 *2.1. Plant material and phenotypic characterization*

90 The data used in this work were obtained with different experiments in two previous studies.  
91 Therefore, our analyses were conducted by separating the methodologies and considering two  
92 datasets: experimental group 1 (EG1) and experimental group 2 (EG2). EG1 includes 408  
93 samples of three F1 segregant populations obtained with crosses between (Pop1) GT1 and  
94 PB235 (30 genotypes) (Souza et al., 2019), (Pop2) GT1 and RRIM701 (127 genotypes) (Conson  
95 et al., 2018; Souza et al., 2019), and (Pop3) PR255 and PB217 (251 genotypes) (Rosa et al.,  
96 2018; Souza et al., 2013, 2019). EG2 is based on an F1 cross between RRIM600 and PB260  
97 (330 samples) (Cros et al., 2019).

98 The parents of the crosses used are important clones for rubber tree breeding programs.  
99 PR255, PB235, PB260, and RRIM600 have high yield, and PB217 has considerable potential  
100 for long-term yield performance due to its slow growth process (Cros et al., 2019; Souza et al.,  
101 2019). PR255 and RRIM701 have good growth, and RRIM701 also presents an increased  
102 SC after initial tapping (Romain & Thierry, 2011). The latex production is stable in PR255  
103 and medium in RRIM600. Stable or medium latex production represents a good adaptation  
104 to several environments, as observed in GT1, a clone tolerant to wind and cold. Additionally,  
105 PB260 presents high female fertility (Baudouin et al., 1997), and PB235 is susceptible to tapping  
106 panel dryness (Sivakumaran et al., 1988).

107 In EG1 and EG2, we analyzed the SC trait. In EG1, Pop3 was planted in 2006 in a  
108 randomized block design in Itiquira, Mato Grosso State, Brazil, 17°24' 03" S and 54°44' 53" W  
109 (Rosa et al., 2018; Souza et al., 2013, 2019). Each individual was represented by four grafted  
110 trees in each plot and four replications. Pop1 and Pop2 were planted in 2012 at the Center of  
111 Rubber Tree and Agroforestry Systems/Agronomic Institute (IAC - Brazil), 20°25' 00" S and  
112 49°59' 00" W, following an augmented block design, with four blocks containing two clones per  
113 plot spaced 4 m apart for each trial, which was repeated four times (Conson et al., 2018; Souza  
114 et al., 2019).

115 Even though EG2 corresponds to only one cross, this population was planted following an  
116 almost complete block design at two different sites (Cros et al., 2019), which for convenience

117 we named site 1 (S1) and site 2 (S2). In S1, 189 clones were planted in 2012 in Société des  
118 Caoutchoucs de Grand-Béréby (SOGB - Ivory Coast), 4°40' 54" N and 7°06' 05" W. In S2, 143  
119 clones were planted in 2013 in Société Africaine de Plantations d'Hévéas (SAPH - Ivory Coast),  
120 5°19' 47.79" N and 4°36' 39.74" W. This cross consisted of six blocks with randomized trees  
121 spaced 2.5 m apart and a mean number of ramets per clone of 11 for S1 (ranging between 7  
122 and 17) and 13 for S2 (ranging between 5 and 20).

123 SC measurements of Pop3 in EG1 were obtained in four years (from 2007 to 2010) and those  
124 of Pop1 and Pop2 were obtained from 2013 to 2016, considering that growth traits are usually  
125 measured only during the first 6 years (Rao & Kole, 2016; Souza et al., 2019). According to  
126 the water distribution of the experiments installed, EG1 phenotypes were measured to supply  
127 information considering low-water (LW) and well-watered (WW) conditions; thus, Pop3 was  
128 evaluated in October 2007-2010 (LW) and in April 2008-2010 (WW), and Pop1 and Pop2 were  
129 evaluated in June 2013, December 2013, May 2014, November 2014, and June 2015-2016. SCs  
130 were measured for individual trees at 50 cm above ground level. For both phenotypes, the  
131 average per plot was calculated. SC in EG2 was measured at 1 m above ground level before  
132 tapping for 3 months every two days except on Sundays (with the beginning at 32 months after  
133 planting in S1 and 38 months after planting in S2).

## 134 *2.2. Phenotypic data analysis*

135 All phenotypic analyses were performed using R statistical software (Team et al., 2013).  
136 EG1 and EG2 traits were analyzed with the following steps: (1) data distribution evaluation;  
137 (2) standardized normalization with the R package bestNormalize (Peterson, 2017); (3) mixed-  
138 effect model creation and residual appropriateness verification through quantile-quantile (Q-Q)  
139 plots using the breedR package (Muñoz & Sanchez, 2019); (4) estimation of best linear unbiased  
140 predictions (BLUPs) based on the models created; (5) hierarchical clustering on BLUP values  
141 using a complete hierarchical clustering approach based on Euclidean distances and dendrogram  
142 visualization with the ggtree R package (Yu et al., 2017); and (6) identification of phenotypic  
143 groups using the clustering approach of (5), with cluster numbers ranging between 2 and 5,  
144 and several clustering indexes implemented in the NbClust R package (Charrad et al., 2014).

145 In EG1, we employed the following statistical mixed-effect model:

$$Y_{ijk} = \mu + L_k + B_{jk} + W + G_{ik} + e_{ijk} \quad (1)$$

146 where  $Y_{ijk}$  corresponds to the phenotype of the  $i$ th genotype in the  $j$ th block and  $k$ th loca-  
147 tion. The phenotypic mean is represented by  $\mu$ , and the fixed effects represent the contribution  
148 of the  $k$ th location ( $L_k$ ), the  $j$ th block at the  $k$ th location ( $B_{jk}$ ), and the watering condition of  
149 the measurement ( $W$ ). The genotype  $G$  and the residual error  $e$  (nongenetic effects) represent  
150 the random effects.

151 EG2 SC phenotypes were modeled for each site (S1 and S2) according to the following  
152 statistical model:

$$Y_{ijk} = \mu + B_j + L_{kj} + R_{rkj} + G_{ij} + e_{ijk} \quad (2)$$

153 where  $Y_{ijk}$  corresponds to the phenotype of the  $i$ th genotype positioned in the  $r$ th rank of  
154 the  $k$ th line in the  $j$ th block. The phenotypic mean is represented by  $\mu$ , and the fixed effects  
155 represent the contribution of the  $j$ th block ( $B_j$ ), the  $k$ th line of the  $j$ th block ( $L_{kj}$ ), and the  
156  $r$ th rank of the  $k$ th line in the  $j$ th block ( $R_{rkj}$ ). The genotype  $G$  and the residual error  $e$   
157 (nongenetic effects) represent the random effects. Broad-sense heritability ( $H^2$ ) was estimated  
158 as  $H^2 = \sigma_g^2 / \sigma_p^2$ , with  $\sigma_g^2$  and  $\sigma_p^2$  representing the genetic and phenotypic variances, respectively.

### 159 2.3. Genotyping process

160 DNA extraction from EG1 was described by Conson et al. (2018); Souza et al. (2013),  
161 and the genotyping process was performed using a genotyping-by-sequencing (GBS) protocol  
162 (Elshire et al., 2011) with *EcoT22I* restriction enzyme followed by Illumina sequencing using  
163 the HiSeq platform for Pop3 and the GAIIX platform for Pop1 and Pop2 (Souza et al., 2019).  
164 Raw sequencing reads were processed using the TASSEL 5.0 pipeline (Glaubitz et al., 2014),  
165 with a minimum count of 6 reads for creating a tag. The tag mapping process was performed  
166 using Bowtie2 v.2.1 (Li & Durbin, 2009) with the *very sensitive* algorithm and *H. brasiliensis*  
167 reference genome (Liu et al., 2020). Single nucleotide polymorphisms (SNPs) were called with  
168 the TASSEL algorithm, and only biallelic SNPs were retained using VCFtools (Danecek et al.,  
169 2011). These markers were filtered using the R package snpReady (Granato et al., 2018b) with

170 a maximum of 20% missing data for a SNP and 50% in an individual and a minimum allele  
171 frequency (MAF) of 5%. Missing data were imputed using the k-nearest neighbors (Cover &  
172 Hart, 1967) algorithm implemented in the snpReady package.

173 EG2 samples were genotyped with simple sequence repeat (SSR) markers, following the  
174 protocol for DNA extraction and genotyping described by Le Guen et al. (2009). A total of 332  
175 SSRs were used for S1 (Tran et al., 2016) and 296 for S2 (Cros et al., 2019). Missing data were  
176 imputed using BEAGLE 3.3.2 (Browning & Browning, 2007) with 25 iterations of the phasing  
177 algorithm and 20 haplotype pairs to sample for each individual in an iteration. The genotypic  
178 profile of individuals in EG1 and EG2 was evaluated using principal component analyses (PCAs)  
179 in R statistical software (Team et al., 2013) with the ggplot2 package (Wickham, 2016).

#### 180 *2.4. Statistical models for genomic prediction*

181 We employed two different strategies for creating traditional genomic prediction models:  
182 Bayesian ridge regression (BRR) (Gianola, 2013) and a single-environment, main genotypic  
183 effect model with a Gaussian kernel (SM-GK) (Cuevas et al., 2016). BRR and SM-GK models  
184 were implemented in the BGLR (Pérez & de Los Campos, 2014) and BGGE (Granato et al.,  
185 2018a) R packages, respectively. Considering the genotype matrix with  $n$  individuals and  $p$   
186 markers, BRR models were implemented considering the following:

$$y = 1\mu + Z\gamma + e \quad (3)$$

187 where  $y$  represents the BLUP values calculated based on the established mixed-effect models  
188 for phenotypic data analyses,  $\mu$  the overall mean,  $Z$  the genotype matrix,  $e$  the residuals, and  
189  $\gamma$  the vector of marker effects. In SM-GK,  $Z$  is the incidence matrix of genetic effects, and  $\gamma$   
190 is the vector of genetic effects with variance estimated through a Gaussian kernel calculated  
191 using the snpReady R package.

#### 192 *2.5. Genomic prediction via machine learning*

193 For genomic prediction via ML, we selected the following algorithms: (a) AdaBoost (Freund  
194 & Schapire, 1997), (b) multilayer perceptron (MLP) neural networks (Popescu et al., 2009),  
195 (c) random forests (Breiman, 2001), and (d) support vector machine (SVM) (Shawe-Taylor &

196 Cristianini, 2000). To create these models, we used Python v.3 programming language together  
197 with the library scikit-learn v.0.19.0 (Pedregosa et al., 2011). We also tested a combination of  
198 feature selection (FS) techniques for increasing the predictive accuracies (Aono et al., 2020),  
199 using a combination of three different methods: (i) L1-based FS through an SVM model (Shawe-  
200 Taylor & Cristianini, 2000), (ii) univariate FS with Pearson correlations (and ANOVA for  
201 discrete variables) (p-value of 0.05), and (iii) gradient tree boosting (Chen & Guestrin, 2016).  
202 Such a strategy is based on marker subset selection, separating the markers identified by all of  
203 these methods together (intersection of the 3 approaches, named Inter3) or by at least two of  
204 them simultaneously (Inter2), and using such subsets for prediction.

205 To understand the subset selection, we performed functional annotation of the genomic re-  
206 gions underlying these markers selected through FS considering a 10,000 base-pair (bp) window  
207 for the up- and downstream regions. Using BLASTn software (Altschul et al., 1990) (minimum  
208 e-value of  $1e-6$ ), these sequences were aligned against coding DNA sequences (CDSs) from  
209 the *Malpighiales* clade (*Linum usitatissimum* v1.0, *Manihot esculenta* v8.1, *Populus deltoides*  
210 WV94 v2.1, *Populus trichocarpa* v4.1, *Ricinus communis* v0.1, and *Salix purpurea* v5.1) of the  
211 Phytozome v.13 database (Goodstein et al., 2012). On the basis of significant correspondence,  
212 Gene Ontology (GO) terms (Botstein et al., 2000) were retrieved.

## 213 2.6. Multilayer perceptron neural network

214 As the final approach for genomic prediction in EG1, we proposed the creation of neu-  
215 ral networks with novel architectures for each of the biparental populations, using the Keras  
216 Python v.3 library for this task (Chollet et al., 2015). We employed MLP networks, which have  
217 an architecture based on multiple layers and feedforward signal propagation (Da Silva et al.,  
218 2017). The MLP architecture is organized into one input layer (IL), followed by at least one  
219 hidden layer (HL) and one output layer (OL). Each one of these layers contains processing ele-  
220 ments, named neurons, which are interconnected with associated unidirectional numeric values  
221 (weights) (Hecht-Nielsen, 1992). The number of neurons in the IL corresponds to the quantity  
222 of explanatory (independent) variables of the problem, which will be propagated across the  
223 MLP structure in one direction (from the input to the output) (Da Silva et al., 2017). The HLs  
224 receive the output of the previous layer until this feedforward propagation generates the OL,

225 respecting the established connections and weights of the architecture. HLs are included in an  
226 MLP to extract unknown patterns from the dataset, making decisions that will contribute to  
227 the overall prediction process (Da Silva et al., 2017; O’Shea & Nash, 2015). After the HLs,  
228 the architecture contains the OL, which is related to the response (dependent) variable of the  
229 problem. For regression tasks with a single output, there is only one neuron in the OL with  
230 linear values (Kurková & Sanguineti, 2013).

231 Each neuron in an MLP has an output value corresponding to impulses that will be propa-  
232 gated into the network. The input signals  $(x_1, x_2, \dots, x_n)$  of a neuron are multiplied by synaptic  
233 weights  $(w_1, w_2, \dots, w_n)$  representing their importance in neuron activation (Da Silva et al.,  
234 2017). The results of these multiplications are aggregated through summation and subtracted  
235 by an activation threshold/bias  $(\theta)$ . Thus, an output signal is produced, whose value is limited  
236 with the use of an activation function  $g$ , e.g., rectified linear activation (ReLU), logistic, arc  
237 tangent, and hyperbolic tangent functions. The purpose of such functions is to introduce non-  
238 linearity into the network (Wang, 2003). The output  $s$  of an HL neuron can then be summarized  
239 in (Da Silva et al., 2017)

$$s = g \left( \sum_{i=1}^n w_i x_i - \theta \right) \quad (4)$$

240 The structure of an artificial neural network is adaptive, changing its conformation during  
241 a process called training, which aims to reach stability in the network via minimal error in pre-  
242 dictive performance through changes in the connection weights (Sheela & Deepa, 2013). The  
243 synaptic weights in an MLP are adjusted by measuring the predictive performance of the ar-  
244 chitecture via an error function, such as the sum of squared errors (Wang, 2003). Even though  
245 the propagation of signals in an MLP is in the forward direction, adjustments of weights are  
246 not propagated in these feedforward connections. Based on the comparison of the network  
247 output with the desirable response and the obtainment of an error value, the weights are  
248 updated in backward propagation (Da Silva et al., 2017) to minimize the found error using  
249 this backpropagation strategy together with an optimization algorithm (Hecht-Nielsen, 1992;  
250 Rumelhart, 1986), such as stochastic gradient descent (SGD), adaptive moment estimation  
251 (Adam) (Kingma & Ba, 2014), and Rmsprop (Bengio, 2015). This process is repeated using

252 the training data in a number of cycles (Hoffer et al., 2017), named epochs, and this backprop-  
253 agation strategy usually employs a batch of samples at each gradient computation for updating  
254 the weights (Hoffer et al., 2019).

255 For all the predictive tasks, we considered an MLP structure with two HLs and used the  
256 mean absolute error (MAE) as the error function for training and defining the architecture  
257 of the networks. Additionally, 200 epochs were considered (batch size of 16). The training  
258 process of the networks was performed using the backpropagation strategy together with the  
259 Adam optimization algorithm (Kingma & Ba, 2014), which aims to minimize the MAE by  
260 updating the synaptic weights using a gradient-based strategy that combines heuristics from  
261 a momentum term and RMSProp (Bengio, 2015). The update process is based on a change  
262 of  $\Delta w_{ij}$  for each connection, considering the individual influence of a weight  $w_{ij}$  on the MAE  
263 value obtained with the gradient descent  $g_t$  in the iteration  $t$  calculated with  $\partial MAE/\partial w_{ij}$  and  
264 used in the equation

$$\Delta w_{ij} = g_t \times \eta \frac{v_t}{\sqrt{s_t + \epsilon}} \quad (5)$$

265 where  $\eta$  is the learning rate representing the amount of change in the process of training,  
266  $v_t$  is the exponential average of gradients along the weights  $w_i$  of layer  $i$ , and  $s_t$  is the ex-  
267 ponential average of squares of gradients along  $w_i$ . The Adam optimizer employs two other  
268 hyperparameters for the optimization process ( $\beta_1$  and  $\beta_2$ ), which are used for the calculation of  
269  $v_t$  ( $v_t = \beta_1 \times v_{t-1} - (1 - \beta_1) \times g_t$ ) and  $s_t$  ( $s_t = \beta_2 \times s_{t-1} - (1 - \beta_2) \times g_t^2$ ). We used  $\beta_1 = 0.9$  and  
270  $\beta_2 = 0.999$  (Kingma & Ba, 2014). We tested the following configurations for the MLP hyperpa-  
271 rameters: (a) number of neurons in the first HL, varying from 1 to  $\sqrt{(q+2)m} + 2\sqrt{m/(q+2)}$   
272 ( $m$  individuals and  $q$  output neurons in the OL); (b) number of neurons in the second HL, vary-  
273 ing from 1 to  $q\sqrt{m/(q+2)}$ ; (c) ReLU, sigmoid and hyperbolic tangent activation functions;  
274 and (d) learning rates of 0.005, 0.001, and 0.0001.

## 275 *2.7. Proposed approach and validation strategies*

276 Each of the sets of hyperparameters estimated for the MLP networks was used to create  
277 a joint and single system for prediction in EG1, which we indicate as part of a divide-and-

278 conquer approach created for genomic prediction (Fig. 1). Considering an individual as part  
 279 of a dataset subpopulation that has a specific phenotypic distribution, we propose the use of a  
 280 two-stage prediction process based on the following steps: (1) creating four different neural net-  
 281 works according to different hyperparameter searches and the training data (division step), (2)  
 282 predicting which subpopulation an unlabeled observation belongs to according to the network  
 283 induced for this task (prediction 1 and conquer step), and (3) predicting its phenotypic perfor-  
 284 mance based on the network trained specifically for the subpopulation predicted (prediction 2  
 285 and final conquer step).

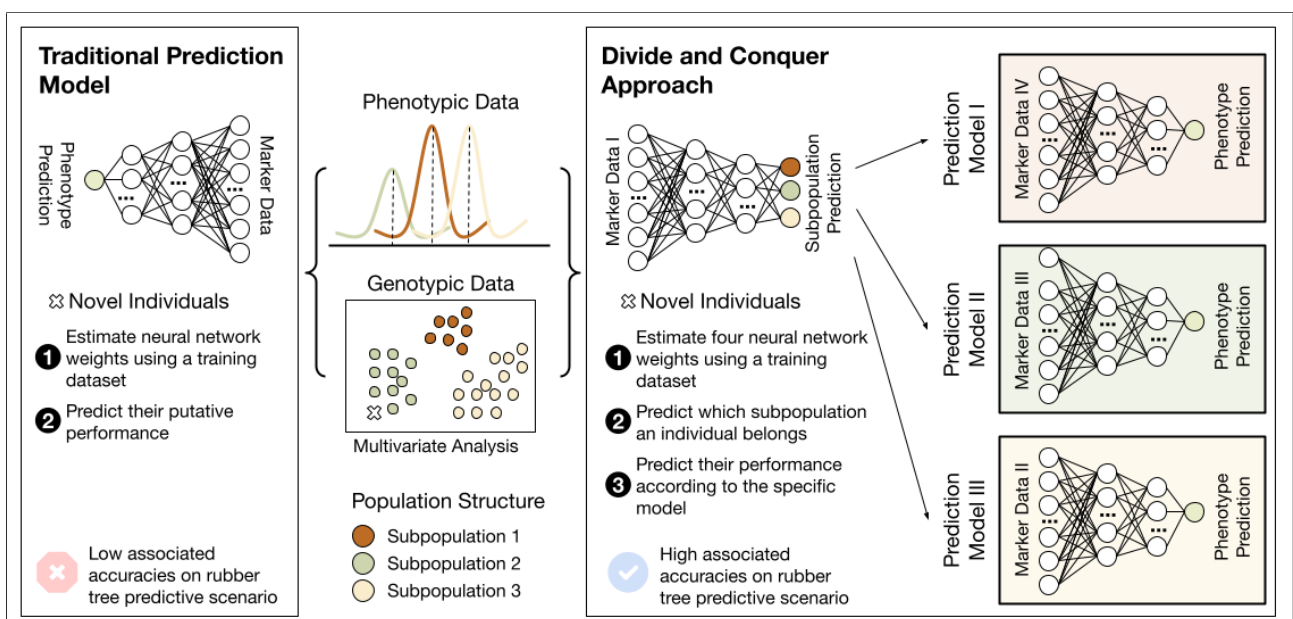


**Fig. 1.** Overview of the approach proposed. Based on a divide-and-conquer strategy with different neural networks combined into a single model (part 1), individuals with unknown phenotypic performance (a) are classified into a subpopulation using a specific neural network (part 2) and (b) have their phenotypic values estimated through an induced network specific to the subpopulation they belong to (part 3).

286 CV1 was the strategy employed for the selection of data for evaluating the models' per-  
 287 formance due to its reduced bias when splitting the dataset and the low prediction accuracies  
 288 described (Souza et al., 2019). We first separated a test dataset using 10% of the genotypes  
 289 with a stratified holdout strategy implemented in the scikit-learn Python v.3 module (Pedregosa  
 290 et al., 2011). The stratification was performed only in EG1 and was based on the subpopulation  
 291 structure present in the dataset. For all the models evaluated in this work (statistical and ML  
 292 based), the same dataset split was considered in every round of CV.

293 The remaining 90% of the genotypes were used as the development set for defining the

294 networks' architecture and for evaluating the overall models' performance through a stratified k-  
295 fold approach (k=4) with 50 repetitions (subpopulation stratification). The predictive accuracy  
296 in every CV split was evaluated by comparing the predicted and real BLUPs by measuring (1)  
297 the Pearson correlation coefficient ( $R$ ) and (2) the mean absolute percentage error (MAPE).  
298 For each trait, we compared the predictive accuracy differences using ANOVA and multiple  
299 comparisons by Tukey's test with the agricolae R package (de Mendiburu & de Mendiburu,  
300 2019).

301 For EG1, four different MLP architectures were estimated: (a) subpopulation prediction, (b)  
302 BLUP prediction for Pop1, (c) BLUP prediction for Pop2, and (d) BLUP prediction for Pop3.  
303 After defining the network hyperparameters with the development set, all of these structures  
304 were joined into a single predictive system that was used for the final prediction. In addition to  
305 evaluating the predictive performance through the CV scenarios created, we also checked the  
306 performance of the model for a leave-one-out (LOO) CV configuration.

### 307 **3. Results**

#### 308 *3.1. Phenotypic and genotypic data analysis*

309 The raw phenotypic data were evaluated considering the experimental groups proposed.  
310 EG1 (Supplementary Fig. 1) had reduced values compared to those of EG2 (Supplementary Fig.  
311 2) due to the different heights and years of stem measurements. However, for the normalized SC  
312 values (Supplementary Figs. 3-5), such an evident discrepancy was not observed. By modeling  
313 the phenotypic measures with the mixed-effect models established and contrasting the raw  
314 values with the normalized ones through Q-Q plots, we observed that the residuals obtained  
315 with the normalized measurements in EG1 (Supplementary Fig. 6) and EG2 (Supplementary  
316 Figs. 7-8) were more appropriate. Heritabilities ( $H^2$ ) were estimated as 0.55 for EG1, 0.83 for  
317 EG2-S1 and 0.93 for EG2-S2, which is in accordance with the findings of Souza et al. (2019)  
318 and Cros et al. (2019).

319 Interestingly, BLUPs from EG1 (Supplementary Fig. 9) and EG2-S1 (Supplementary Fig.  
320 10) presented reduced variability when compared to that of BLUPs estimated for EG2-S2 (Sup-  
321 plementary Fig. 10). This observation is corroborated by the hierarchical clustering analyses

322 performed for these experimental groups. EG1 (Supplementary Fig. 11) and EG2-S1 (Supple-  
323 mentary Fig. 12) could be divided into three phenotypic groups according to the best data  
324 partitioning scheme established through NbClust clustering indexes (Charrad et al., 2014), and  
325 EG2-S2 could be arranged into 5 such groups (Supplementary Fig. 13). Therefore, it was  
326 expected that for the genomic prediction step, EG2-S2 would represent a more difficult task  
327 due to its higher data variability.

328 SNP calling in EG1 was performed according to the TASSEL pipeline. Of the 363,641 tags  
329 produced, approximately 84.78% could be aligned against the *H. brasiliensis* reference genome,  
330 which generated 107,466 SNPs. These markers were filtered separately for each population  
331 using the parameters established, and then these separated datasets were combined through  
332 intersection comparisons, yielding a final dataset of 7,414 high-quality SNP markers. For EG2  
333 predictions, 332 and 296 SSR markers were used for EG2-S1 and EG2-S2, respectively.

334 Using these datasets, we performed PCAs for EG1 (Supplementary Fig. 14) and EG2 (Sup-  
335 plementary Fig. 15). In the figures, the colors of the genotypes correspond to their BLUP  
336 values, and their shapes correspond to population structure in EG1 and site in EG2. As  
337 expected, for the SC trait, there were no clear associations between markers and BLUPs, un-  
338 derlining the challenge of creating genomic prediction models. Additionally, the subpopulation  
339 structure in EG1 was evident.

### 340 3.2. Genomic prediction

341 From the BLUP and marker datasets, we fit genomic prediction models using the traditional  
342 statistical approaches (BRR and SM-GK) and the ML algorithms (AdaBoost, MLP, RF, and  
343 SVM) selected. For EG1 (Supplementary Fig. 16), EG2-S1 (Supplementary Fig. 17) and  
344 EG2-S2 (Supplementary Fig. 18), no substantial changes were observed when changing the  
345 prediction approach. After applying Tukey's multiple comparisons test, we found equivalent  
346 performance values for SVM, SM-GK and BRR for all the experimental groups. The worst  
347 performance was observed for MLP, however, considering the default architectures employed in  
348 scikit-learn (Pedregosa et al., 2011).

349 Additionally, we also tested the inclusion of FS techniques for increasing model performance  
350 in ML algorithms. Using the Inter2 approach, we selected 539 (~7.27%), 69 (~20.78%) and

351 82 (~27.70%) markers for EG1, EG2-S1 and EG2-S2, respectively. For Inter3, 113 (~1.52%),  
352 8 (~2.41%) and 15 (~5.07%) markers were identified. This SNP subsetting approach was  
353 beneficial for EG1 (Supplementary Fig. 19A), EG2-S1 (Supplementary Fig. 20) and EG2-S2  
354 (Supplementary Fig. 21); however, there were less pronounced improvements for data from  
355 EG2 sites, which was expected because of the limited SSR marker dataset. We considered  
356 that, even with increased predictive accuracies, to achieve better results, a wider set of markers  
357 would be required. Then, we considered the best strategy for EG2-S1 to be the combination  
358 of the Inter2 FS approach with SVM and that for EG2-S2 to be the combination of Inter3 FS  
359 with the AdaBoost ML algorithm.

360 Even though FS approaches boosted prediction accuracies for EG1, when analyzing model  
361 performance by calculating the Pearson correlation between the real and predicted BLUPs for  
362 each family separately, this better performance was caused by the overall predictions. However,  
363 when analyzing predictive power within families (Supplementary Fig. 19B), such an approach  
364 was not sufficient for obtaining a reliable prediction with this evident data stratification. In  
365 this context, different from EG2, we developed an approach specific to datasets similar to EG1,  
366 i.e., a methodology with high capabilities to supply accurate predictions, even considering the  
367 subpopulation structure present in a dataset.

368 Considering a genomic prediction problem based on the creation of a regression model for a  
369 dataset containing genotypes that belong to different groups of genetically similar individuals,  
370 we modeled such a task by dividing the prediction into different stages (Fig. 1) and creating  
371 a divide-and-conquer approach for prediction. The basis of such an approach is that closely  
372 related genotypes will share QTLs that might not be the same in another group of genotypes.  
373 Therefore, we created a different neural network for each biparental population (divide part),  
374 coupled with an intrapopulation system of FS and with a different form of hyperparameter esti-  
375 mation. Following this division part, the separated systems were combined using an additional  
376 step (the conquer part). To do so, another neural network was created to infer which subpart  
377 of the system should be used for prediction.

378 *3.3. Feature selection at the subpopulation level*

379 The selection of subsets of markers was performed according to each EG1 network using  
380 the four different tasks: (i) subpopulation prediction, (ii) EG1-Pop1 BLUP prediction, (iii)  
381 EG1-Pop2 BLUP prediction, and (iv) EG1-Pop3 BLUP prediction. As expected, each FS  
382 strategy returned a different quantity of markers (Table 1). For each subset of markers selected  
383 considering Inter2 and Inter3, we evaluated their performance using the ML algorithms selected.  
384 Some of the models created for task (i) did not present any mistakes (Supplementary Fig. 22),  
385 which was expected due to the subpopulation structure present in the dataset and their evident  
386 linear separability. For this task, we considered the most suitable FS strategy to be the Inter2  
387 approach.

**Table 1**

Feature selection strategies performed on the marker dataset considering the intersection among the three methods established (Inter3) and the intersection among at least two out of the three methods established (Inter2).

Prediction Scenario	Inter2	Inter3
Subpopulation Prediction	224	17
GT1 x PB235	345	20
GT1 x RRIM701	454	62
PR255 x PB217	591	119

388 For EG1-Pop1 (Supplementary Fig. 23), EG1-Pop2 (Supplementary Fig. 24) and EG1-Pop3  
389 (Supplementary Fig. 25), the best accuracies were observed for the combination Inter2-SVM.  
390 However, considering the overall performance with the other algorithms, the best approach for  
391 SNP subsetting was Inter3. For this reason, we selected this strategy for the BLUP predic-  
392 tion task. Interestingly, there was no intersection between these three Inter3 datasets in the  
393 populations; the only case of overlap was a single SNP marker in Pop2 and Pop3.

394 From the genomic regions flanking these markers selected for BLUP prediction, we could  
395 retrieve several instances of correspondence between rubber tree sequences and CDSs from  
396 the *Malpighiales* clade in the Phytozome database. From the 20 markers used in Pop1 for  
397 prediction, 62 in Pop2, and 119 in Pop3, we found CDS correspondence for the genomic regions  
398 related to 8 (40%), 27 (~43.55%) and 48 (~40.32%) SNPs, respectively. Even though there was  
399 no obvious complementarity among these markers due to the absence of intersections, we found

400 GO terms with similar biological processes (Supplementary Tables 1-3), indicating common  
401 molecular processes related to these genomic regions.

### 402 3.4. Neural network creation

403 With the marker dataset established through FS for EG1 subtasks, we estimated the best  
404 hyperparameter configuration for creating the networks proposed: (i) subpopulation predic-  
405 tion in EG1 (Supplementary Fig. 26), (ii) BLUP prediction in EG1-Pop1 (Supplementary Fig.  
406 27), (iii) BLUP prediction in EG1-Pop2 (Supplementary Fig. 28), and (iv) BLUP prediction in  
407 EG1-Pop3 (Supplementary Fig. 29). With the exception of network (i), which is a classification  
408 task, for each hyperparameter combination, we evaluated the MAPE and R Pearson coefficient  
409 values using the development set to select the best configuration for prediction. For network (i),  
410 several hyperparameter combinations returned prediction capabilities without mistakes (Sup-  
411 plementary Fig. 26), which led us to select the configuration with the minimum value for the  
412 loss function (Table 2).

**Table 2**

Hyperparameter definition for each one of the created neural networks in experimental groups 1 (EG1) and 2 (EG2) considering (i) the number of neurons selected for the first hidden layer (N-1HL), (ii) the number of neurons selected for the second hidden layer (N-2HL), (iii) the learning rate (LR), and (iv) the activation function (AF).

Neural Network	N-1HL	N-2HL	LR	AF
EG1 (Subpopulation Prediction)	45	25	0.005	Rectified linear activation
EG1 (BLUP Prediction in GT1 x PB235)	10	3	0.005	Rectified linear activation
EG1 (BLUP Prediction in GT1 x RRIM701)	30	7	0.005	Rectified linear activation
EG1 (BLUP Prediction in PR255 x PB217)	42	4	0.005	Rectified linear activation

413 For networks (ii), (iii) and (iv), we selected the best hyperparameter combination by eval-  
414 uating the plot profiles. We selected the combinations closest to the right corner of the plots  
415 (Supplementary Figs. 27-29), ideally representing the best MAPE and R Pearson coefficient  
416 simultaneously. Interestingly, for the four networks, the best activation function was ReLU,  
417 and the learning rate was 0.005, only changing the quantity of neurons in the established HLs.  
418 An evaluation of the predictive performance of these networks compared to the traditional ge-  
419 nomic prediction approaches with k-fold CV built in the development set revealed significant  
420 improvement and effective performance in each population, different from the FS performed  
421 using these datasets combined (Supplementary Fig. 19).

422 The network modeled for EG1-Pop1 showed the largest increases (Supplementary Fig. 30),  
423 with a mean improvement of 9 times the initial obtained accuracies. EG1-Pop2 (Supplementary  
424 Fig. 31) and EG1-Pop3 (Supplementary Fig. 32) showed increases of 7 and 3 times, respec-  
425 tively. In addition to such significant improvements, the models' performance was also more  
426 stable, with the predictive accuracies having a narrow distribution, as observed in the boxplots'  
427 conformations.

### 428 3.5. Divide-and-conquer approach

429 All of the individual networks were combined to create the proposed approach in EG1.  
430 Compared with the traditional approaches, this approach showed a mean improvement of 4  
431 times the initial accuracies (Fig. 2A) in the k-fold evaluations. Moreover, BRR and SM-GK  
432 presented equivalent performance values. Additionally, when analyzing the performance of  
433 the development set for predicting the BLUP values of genotypes from the test set, we found  
434 Pearson R coefficients of 0.39, 0.42, and 0.81 for BRR, SM-GK, and the proposed approach,  
435 respectively, showing the methodology's efficiency even for data not in the development set.

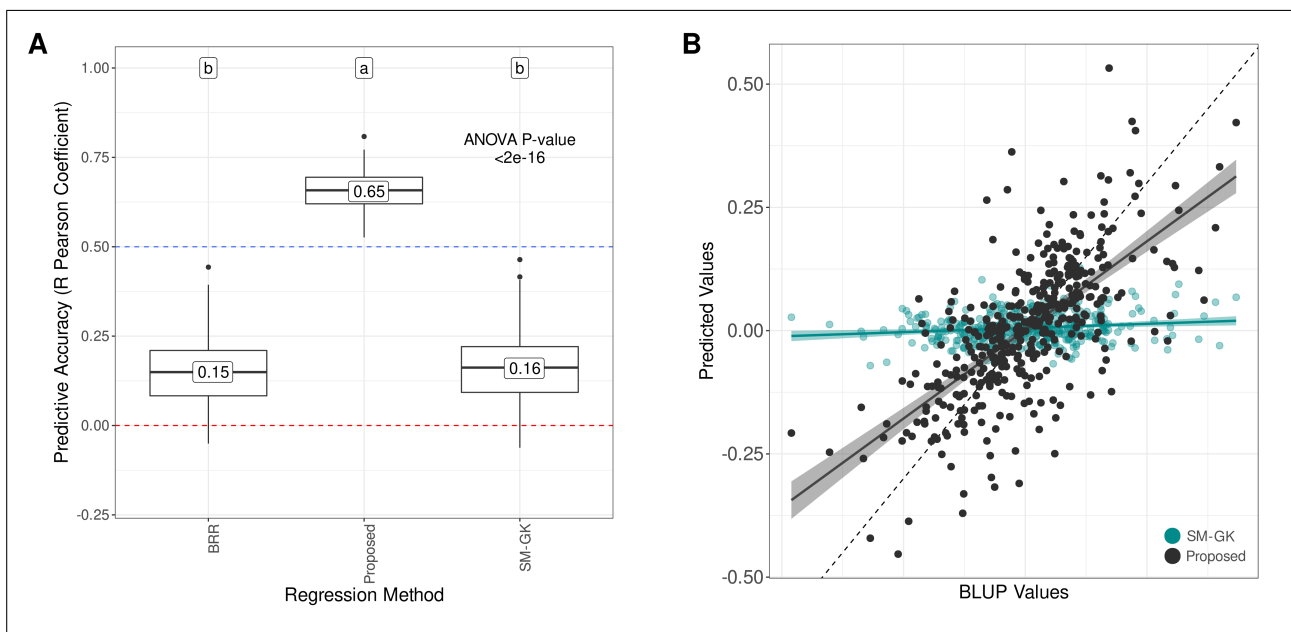


**Fig. 2.** Predictive accuracies for stem circumference BLUP prediction in experimental group 1 (EG1) considering (A) a 4-fold cross validation (CV) scheme (50 times repeated) and (B) a leave-one-out CV strategy. The models used for prediction were a single-environment model with a nonlinear Gaussian kernel (SM-GK), Bayesian ridge regression (BRR), and the proposed strategy using the divide-and-conquer approach. The labels indicate the results from Tukey's multiple comparison test.

436 As the final step in model evaluation, we performed a LOO CV split to check whether

437 an increase in the training data improves prediction accuracy. By contrasting the real BLUP  
438 values with the predicted values, we found R Pearson coefficients of 0.14, 0.16 and 0.68 for  
439 BRR, SM-GK, and the proposed approach, respectively. The regression curve clearly indicates  
440 the proposed approach's appropriateness for rubber tree data (Fig. 2B).

#### 441 4. Discussion

442 GS has emerged as a potential tool for application in plant breeding programs (Cros et al.,  
443 2015; Crossa et al., 2016; O'Connor et al., 2018; Spindel et al., 2015; Wolfe et al., 2017; Xavier  
444 et al., 2016; Zhao et al., 2012). In rubber tree, previously obtained results (Cros et al., 2019;  
445 Souza et al., 2019) have demonstrated the potential of such a technique for reducing breeding  
446 cycles. Because of the strong commercial rubber demand, there have been many economic  
447 incentives for rubber tree production in more environments beyond its natural range (Ahrends  
448 et al., 2015; Warren-Thomas et al., 2015). Considering the difficulty of achieving ideal condi-  
449 tions for cultivating *H. brasiliensis* and the rubber demand, the development of more efficient  
450 varieties is needed. However, *Hevea's* long life cycle considerably reduces breeding efficiency  
451 (An et al., 2019). Therefore, the application of GS in rubber tree represents an alternative for  
452 achieving the desired rubber production in less time by replacing clone trials and reducing the  
453 long period of phenotypic evaluation (Cros et al., 2019).

454 The main objective of rubber tree breeding programs is to increase latex production with  
455 rapid growth (Rosa et al., 2018). Increased SC development can be associated with several rub-  
456 ber tree characteristics, such as growth (Chandrashekar et al., 1998), latex production (Souza  
457 et al., 2019), and drought resistance (Zhang et al., 2019). Due to the high versatility of SC  
458 in evaluating rubber trees (Chanroj et al., 2017; Dijkman et al., 1951; Gonçalves et al., 1984;  
459 Khan et al., 2018), we proposed to develop more effective models for predicting this trait, pro-  
460 viding a method to be incorporated into the estimation of tree performance. The lack of high  
461 genotype variability in the datasets used represents a real scenario for rubber tree breeding  
462 programs (Souza et al., 2019), which face the difficulty of generating a population (Cros et al.,  
463 2019). In addition to the within-family approach suggested for GS with full-sib families by  
464 Cros et al. (2019), the use of interconnected families is a common strategy for perennial species

465 (Grattapaglia, 2017; Kumar et al., 2015; Muranty et al., 2015).

466 Using these dataset configurations, we evaluated ML algorithms as a more accurate method-  
467 ology for predicting SC, a complex trait. Cros et al. (2019) obtained a mean accuracy for rubber  
468 production in a CV0 scenario of 0.53, which increased to 0.56 when selecting a set of markers  
469 based on heterozygosity values. In a CV1 scheme, the mean values ranged between 0.33 and  
470 0.60. In the proposed work, we observed even lower accuracies when using SC instead of rubber  
471 production, which is in accordance with the findings of Souza et al. (2019). In (Souza et al.,  
472 2019), the authors achieved mean accuracies ranging between 0.19 and 0.28 in a CV1 scenario,  
473 contrasted with a CV2 scheme with values ranging between 0.84 and 0.86. For unknown tested  
474 genotypes, the predictive accuracies in rubber tree are low, and the inclusion of GS in *Hevea*  
475 breeding programs is therefore still not feasible.

476 Using the traditional approaches for prediction, we achieved LOO configurations of 0.14  
477 and 0.16 for the BRR and SM-GK approaches, respectively, which is similar to what Souza  
478 et al. (2019) observed. The BRR and SM-GK methodologies were selected to represent a  
479 parametric and a semiparametric approach (Heslot et al., 2012). Different from BRR, which  
480 estimates marker effects, SM-GK estimates genotype effects through a relationship matrix  
481 obtained with a reproducing kernel (Granato et al., 2018a). Even though Souza et al. (2019)  
482 found similar results when using a linear and a nonlinear kernel for the estimation of the genomic  
483 relationship matrix, Gianola et al. (2014) considered GK to have a more flexible structure and  
484 a higher associated performance. Therefore, considering these findings together with the fact  
485 that no significant differences have been found among statistical models for GS (Ma et al.,  
486 2018; Roorkiwal et al., 2016; Varshney, 2016), we selected only these two statistical models for  
487 predictive evaluation.

488 Even though some previous attempts did not reveal significant differences in employing  
489 ML in GS compared with traditional linear regression methodologies (Crossa et al., 2019;  
490 Montesinos-López et al., 2019a, 2018, 2019b; Zingaretti et al., 2020), this is not what we ob-  
491 served in our study, which corroborates the findings of Bellot et al. (2018); Liu et al. (2019);  
492 Ma et al. (2018); Waldmann et al. (2020). This discrepancy may be explained by the different  
493 strategies used in the ML algorithms, especially distinct neural network architectures, training

494 methodologies, and CV scenarios. The design of neural network architectures is an important  
495 step in using deep learning for prediction because differences in the definition of topologies can  
496 lead to decreased accuracies (Ma et al., 2018).

#### 497 *4.1. Divide-and-conquer strategy*

498 Several factors are known to influence prediction accuracy in GS, such as the relationship  
499 between the individuals used to train models and those that will be predicted (Washburn et al.,  
500 2019), the size and structure of the populations used (Crossa et al., 2017), the trait heritability  
501 (Zhang et al., 2017), the marker density (Liu et al., 2018), and the linkage disequilibrium (LD)  
502 between the set of markers used and the associated QTLs (Raymond et al., 2018). This last  
503 aspect is especially critical in the datasets employed because of the limited set of markers  
504 obtained through GBS and SSR genotyping. Considering the reduced accuracies obtained with  
505 the CV1 technique already described in (Cros et al., 2019; Souza et al., 2019), it was expected  
506 that when using a K-fold strategy, the same observations would be found for the traditional  
507 regression models.

508 One of the main challenges in GS is the high dimensionality of the features in the datasets  
509 because the number of SNPs is much larger than the number of phenotypic observations (Long  
510 et al., 2007) ('large  $p$ , small  $n$ ' problem). Although a greater saturation of markers enables an  
511 increase in the probability of finding LD, a larger number of markers in the same LD block  
512 does not contribute to better prediction performance (Liu et al., 2018). In this context, FS  
513 techniques may be an alternative strategy for building a predictive model, considering that  
514 not all markers are related to a specific phenotype (Yin et al., 2019) and that the quantity  
515 required for this task directly depends on the complexity and genetic architecture of the traits  
516 used (Liu et al., 2018). Therefore, like Bermingham et al. (2015), Bellot et al. (2018), Li et al.  
517 (2018), Inácio & Alves (2019), Aono et al. (2020), Ramzan et al. (2020), Luo et al. (2021), and  
518 Pimenta et al. (2021), we decided to test the prediction improvements by using an FS technique  
519 to enhance network performances.

520 Subset selection showed improvements for EG2 (Supplementary Figs. 20-21); however,  
521 there were no sizable improvements because of the genetic complexity of SC (Francisco et al.,  
522 2021) and the low density of SSR markers (Nadeem et al., 2018). In EG1, although an overall

523 improvement in prediction accuracy was observed (Supplementary Fig. 19), when evaluating  
524 the intrapopulation predictive accuracy, we observed clear inefficiency of the approach, probably  
525 caused by the different allele substitution effects between the three subpopulations employed  
526 (Raymond et al., 2018). In such a scenario with unbalanced interconnected families, novel  
527 approaches are needed, and in this work, we have proposed the use of a divide-and-conquer  
528 strategy.

529 In computer science, the divide-and-conquer paradigm is based on the principle that if a  
530 problem is not simple enough to be solved directly, it can be divided into subproblems, and  
531 their results can be combined (Smith, 1985). In our prediction task, the BLUPs of the popu-  
532 lations could not be properly predicted together; thus, we separated the problem into different  
533 networks for prediction, combining the strategy into a single network structure. Such an ap-  
534 proach has already been applied to the development of neural network architectures (Feng  
535 et al., 2019; Frosyniotis et al., 2003; Mohamad, 2013; Sakhakarmi & Park, 2020); however, such  
536 a formulation has not been explored in genomic prediction. In addition to increasing prediction  
537 accuracies, such an approach can reduce the time required for network training and hyperpa-  
538 rameter estimation (Mohamad, 2013), supply superior model interpretability without loss of  
539 performance (Fu et al., 2019), and be used in combination with other models (Intanagonwiwat,  
540 1998), including traditional genomic prediction methods. Considering that in genomic predic-  
541 tion, most of the scenarios include different population structures, such a paradigm can benefit  
542 the application and development of GS strategies.

543 In our dataset, most of the observed variance within SNP markers was caused by population  
544 structure, which is clearly shown by the PCA results (Supplementary Fig. 14). As this strong  
545 variability can be associated with several genomic regions and influence various traits differently  
546 and simultaneously in the populations (Linhart & Grant, 1996), we hypothesize that traditional  
547 genomic prediction models are not capable of capturing these interpopulation differences related  
548 to SC QTLs. This is the main reason why performing FS on these unbalanced datasets together  
549 was not a promising strategy in our study. As intrapopulation QTLs are not transferable to  
550 other populations, the main effects on phenotypic variation are specific to the within-population  
551 genetic structure (Würschum, 2012). In this sense, the prediction task in single populations can

552 be seen as simpler than that in multiple populations (Ogut et al., 2015), which was the basis for  
553 developing the divide-and-conquer strategy. Considering the specific effects of causal genetic  
554 variants within populations (Hirschhorn et al., 2001; Pressoir & Berthaud, 2004), we tried to  
555 incorporate such factors into separate networks with their specific hyperparameter optimization  
556 processes.

557 Interestingly, FS steps performed in the three different populations of EG1 returned different  
558 markers, but these markers were putatively associated with genes acting in similar biological  
559 processes. GO mRNA splicing was found in the intersection set of markers selected for the  
560 three populations. The occurrence of genetic variation related to such a regulatory process  
561 may influence the transcription of diverse mRNAs from the same gene in different ways. Such  
562 diversity of molecules may be related to differences in phenotypic performance, leading to  
563 increased plant capabilities (Mastrangelo et al., 2012; Szakonyi & Duque, 2018; Wei et al.,  
564 2017). Additionally, base-excision repair was found in both Pop1 and Pop3, which represents a  
565 very important defense pathway for maintaining genomic integrity (Roldán-Arjona et al., 2019)  
566 and is clearly essential for rubber tree growth and development (Murphy, 2005). Due to the  
567 increased quantity of individuals in Pop2 and Pop3, more GO categories were found, including  
568 important processes for plant growth, such as response to different types of stress and several  
569 metabolic processes (Francisco et al., 2021).

#### 570 *4.2. Deep learning architectures*

571 Different studies have reported the use of deep learning for genomic prediction with various  
572 datasets, including for humans (Bellot et al., 2018; Yin et al., 2019), sows (Waldmann et al.,  
573 2020), and plant species such as soybean (Liu et al., 2019), wheat (Crossa et al., 2019; Ma et al.,  
574 2018; Montesinos-López et al., 2019a, 2018, 2019b), maize (Montesinos-López et al., 2018), and  
575 strawberry and blueberry (Zingaretti et al., 2020). Even though all of these studies used deep  
576 learning, the neural network creation approaches were not the same; some of them included  
577 architectures of convolutional neural networks (CNNs) (Waldmann et al., 2020; Yin et al.,  
578 2019; Zingaretti et al., 2020), while others included MLPs (Crossa et al., 2019; Montesinos-  
579 López et al., 2019a, 2018, 2019b) or both approaches (Bellot et al., 2018; Liu et al., 2019; Ma  
580 et al., 2018). There is no consensus on the efficiency of neural networks for genomic prediction;

581 however, we decided to use such an architecture for combining multiple training processes into  
582 a single predictive structure.

583 For each of the neural network architectures, we employed an MLP structure. We did not  
584 include convolutional operations because of the reduced quantity of markers obtained through  
585 FS. Additionally, CNNs were developed for extracting unknown patterns from the dataset, and  
586 as we hypothesized that FS operations might work as indicators of QTL regions, such operations  
587 would not be necessary. To define the most promising network architecture, we used a grid  
588 search, testing different combinations of hyperparameters as already performed in relation to  
589 GS strategies (Crossa et al., 2019; Montesinos-López et al., 2019a, 2018, 2019b). Although other  
590 researchers have used the ‘trial and error’ approach to define the network topology (Sheela &  
591 Deepa, 2013), we preferred to develop a strategy that could be replicated in other predictive  
592 scenarios, especially with other traits and crops.

593 The approximation of functions through neural networks was supported first based on Kol-  
594 mogorov (1957) and later on Hecht-Nielsen (1987), which extended the theorem of Kolmogorov  
595 (1957), proving that any continuous function can be represented by a neural network with one  
596 HL containing  $2n + 1$  nodes ( $n$  features) and a more complex activation function than that  
597 usually employed by current researchers (Stathakis, 2009). It has already been proven that one  
598 HL is capable of universal approximation by using a complex activation function (Hornik, 1993;  
599 Hornik et al., 1989; Huang, 2003; Thomas et al., 2017; Wang, 2003); however, when using regu-  
600 lar functions, such as sigmoid and ReLU functions, there is reduced efficiency of such networks.  
601 In this context, Kurková (1992) suggested that two HLs could be a solution for this reduced  
602 efficiency. In addition, the usage of an additional HL can substantially reduce the total number  
603 of required nodes for a satisfactory predictive capability (Stathakis, 2009), and it has already  
604 been shown that some problems can be solved only by the use of two HLs (Chester, 1990; Son-  
605 tag, 1991; Thomas et al., 2017). In practical situations, a neural network architecture with two  
606 HLs generalizes better than that with one and has been considered a superior approach (Islam  
607 & Murase, 2001; Thomas et al., 2017). Therefore, in our study, we decided to include two HLs  
608 in our proposed architecture, representing a network with more complex training complexity  
609 (Kurková & Sanguineti, 2013).

610 Concerning the quantity of hidden neurons in a neural network, many researchers have  
611 developed different strategies, aiming at increasing accuracy and prediction while decreasing  
612 errors (Sheela & Deepa, 2013). Huang (2003) has already proven that in a network architecture  
613 with two HLs, the number of nodes required to achieve a reasonable predictive accuracy with  $m$   
614 samples and  $q$  output neurons is  $\sqrt{(q+2)m} + 2\sqrt{m/(q+2)}$  in the first HL and  $q\sqrt{m/(q+2)}$   
615 in the second HL. However, the quantity of suggested nodes tends to lead to overfitting of  
616 the training data with any arbitrary small error (Sheela & Deepa, 2013), and considering the  
617 capability of predicting unknown data, these values can be considered the maximum number of  
618 nodes in an artificial neural network structure (Stathakis, 2009). The lower bound for hidden  
619 neurons was already proposed by Jiang et al. (2008), which can be useful for accelerating the  
620 learning speed, but there was no evidence on separating this quantity across HLs, and the study  
621 was based on an MLP with 3 HLs (Sheela & Deepa, 2013). Thus, in our architecture definition,  
622 we decided to test a large quantity of neurons, considering the findings of Huang (2003), as our  
623 upper bound.

624 The created network coupling the population-specific architectures could increase the ini-  
625 tial prediction capabilities by more than four times. Such an improvement represents the first  
626 attempt to develop a ML strategy for genomic prediction in rubber tree, with a high potential  
627 to be adapted to other species with the same data configuration. Considering a broader sce-  
628 nario with distantly related genotypes belonging to a population with undefined structure, this  
629 same approach could be applied. Instead of relying on the predefined stratification, clustering  
630 analyses could be performed and used for the divide part. Such a practice is already common  
631 in breeding, i.e., taking advantage of population structure for model prediction through multi-  
632 variate techniques (Berro et al., 2019; Guo et al., 2014; Stewart-Brown et al., 2019; Wang et al.,  
633 2017). Taking into account the importance of such group configuration in the differentiation of  
634 multiple traits (Bolnick et al., 2011; Goodnight, 1989; Merilä & Crnokrak, 2001), the strategy  
635 developed represents a promising approach for several plant species with a difficult prediction  
636 scenario.

637 The use of GS in rubber tree can optimize breeding programs, and the incorporation of  
638 ML techniques can be seen as a new possibility for building more robust models with higher

639 associated prediction capabilities. By using data from rubber tree breeding programs, we were  
640 able to generate promising predictive results for a highly complex trait and a novel strategy for  
641 prediction, which has significant potential to enhance selection efficiency, reduce the length of  
642 the selection cycle, and supply a means of developing low-density markers to be employed in  
643 MAS because of the FS steps. Although our results confirmed the efficiency of the methodology  
644 proposed for rubber tree data, to properly evaluate the full potential of the method in other  
645 species and broader scenarios, our approach should be investigated in further studies with more  
646 genetically diverse populations in contrasting environments.

### 647 **Author contributions**

648 AA and FF performed all the analyses and wrote the manuscript; PG, EJ and VG conducted  
649 the field experiments; LS, RF, MQ, GG and AS conceived the project. All authors reviewed,  
650 read and approved the manuscript.

### 651 **Acknowledgements**

652 The authors gratefully acknowledge the Fundação de Amparo à Pesquisa do Estado de São  
653 Paulo (FAPESP) for Ph.D. fellowships to FF (2018/18985-7) and AA (2019/03232-6) and for  
654 a research internship abroad (BEPE) scholarship to AA (2019/26858-8), the Coordenação de  
655 Aperfeiçoamento do Pessoal de Nível Superior (CAPES) for financial support (Computational  
656 Biology Program and CAPES-Agropolis Program), and the Conselho Nacional de Desenvolvi-  
657 mento Científico e Tecnológico (CNPq) for research fellowships to AS and PG.

### 658 **Data availability statement**

659 The genotypic data from EG1 are available under NCBI accessions PRJNA540286 (ID:  
660 5440286) (GT1 × PB235 and GT1 × RRIM701) and PRJNA541308 (ID: 541308) (PR255 ×  
661 PB217). The datasets from EG2 were made available by Cros et al. (2019).

## 662 References

- 663 Ahrends, A., Hollingsworth, P. M., Ziegler, A. D., Fox, J. M., Chen, H., Su, Y., & Xu, J., 2015.  
664 Current trends of rubber plantation expansion may threaten biodiversity and livelihoods.  
665 *Global Environ. Change*, *34*, 48–58.
- 666 Albrecht, T., Wimmer, V., Auinger, H.-J., Erbe, M., Knaak, C., Ouzunova, M., Simianer, H.,  
667 & Schön, C.-C. (2011). Genome-based prediction of testcross values in maize. *Theor. Appl.*  
668 *Genet.*, *123*, 339.
- 669 Altschul, S. F., Gish, W., Miller, W., Myers, E. W., & Lipman, D. J., 1990. Basic local  
670 alignment search tool. *J. Mol. Biol.*, *215*, 403–410.
- 671 An, Z., Zhao, Y., Zhang, X., Huang, X., Hu, Y., Cheng, H., Li, X., & Huang, H., 2019. A  
672 high-density genetic map and qtl mapping on growth and latex yield-related traits in hevea  
673 brasiliensis müll. arg. *Ind. Crops Prod.*, *132*, 440–448.
- 674 Aono, A. H., Costa, E. A., Rody, H. V. S., Nagai, J. S., Pimenta, R. J. G., Mancini, M. C.,  
675 Dos Santos, F. R. C., Pinto, L. R., de Andrade Landell, M. G., de Souza, A. P. et al., 2020.  
676 Machine learning approaches reveal genomic regions associated with sugarcane brown rust  
677 resistance. *Sci. Rep.*, *10*, 1–16.
- 678 Baudouin, L., Baril, C., Clément-Demange, A., Leroy, T., & Paulin, D., 1997. Recurrent  
679 selection of tropical tree crops. *Euphytica*, *96*, 101–114.
- 680 Bellot, P., de los Campos, G., & Pérez-Enciso, M., 2018. Can deep learning improve genomic  
681 prediction of complex human traits? *Genetics*, *210*, 809–819.
- 682 Bengio, Y., 2015. Rmsprop and equilibrated adaptive learning rates for nonconvex optimization.  
683 *corr abs/1502.04390*.
- 684 Bermingham, M. L., Pong-Wong, R., Spiliopoulou, A., Hayward, C., Rudan, I., Campbell, H.,  
685 Wright, A. F., Wilson, J. F., Agakov, F., Navarro, P. et al., 2015. Application of high-  
686 dimensional feature selection: evaluation for genomic prediction in man. *Sci. Rep.*, *5*, 1–12.

- 687 Bernardo, R., & Yu, J., 2007. Prospects for genomewide selection for quantitative traits in  
688 maize. *Crop Sci.*, *47*, 1082–1090.
- 689 Berro, I., Lado, B., Nalin, R. S., Quincke, M., & Gutiérrez, L., 2019. Training population  
690 optimization for genomic selection. *Plant Genome*, *12*, 190028.
- 691 Bolnick, D. I., Amarasekare, P., Araújo, M. S., Bürger, R., Levine, J. M., Novak, M., Rudolf,  
692 V. H., Schreiber, S. J., Urban, M. C., & Vasseur, D. A., 2011. Why intraspecific trait  
693 variation matters in community ecology. *Trends Ecol. Evol.*, *26*, 183–192.
- 694 Botstein, D., Cherry, J. M., Ashburner, M., Ball, C. A., Blake, J. A., Butler, H., Davis, A. P.,  
695 Dolinski, K., Dwight, S. S., Eppig, J. T. et al., 2000. Gene ontology: tool for the unification  
696 of biology. *Nat. Genet.*, *25*, 25–9.
- 697 Breiman, L., 2001. Random forests. *Mach. Learn.*, *45*, 5–32.
- 698 Browning, S. R., & Browning, B. L., 2007. Rapid and accurate haplotype phasing and missing-  
699 data inference for whole-genome association studies by use of localized haplotype clustering.  
700 *Am. J. Hum. Genet.*, *81*, 1084–1097.
- 701 Chandrashekar, T., Nazeer, M., Marattukalam, J., Prakash, G., Annamalainathan, K., &  
702 Thomas, J., 1998. An analysis of growth and drought tolerance in rubber during the imma-  
703 ture phase in a dry subhumid climate. *Exp. Agric.*, *34*, 287–300.
- 704 Chanroj, V., Rattanawong, R., Phumichai, T., Tangphatsornruang, S., & Ukoskit, K., 2017.  
705 Genome-wide association mapping of latex yield and girth in amazonian accessions of hevea  
706 brasiliensis grown in a suboptimal climate zone. *Genomics*, *109*, 475–484.
- 707 Charrad, M., Ghazzali, N., Boiteau, V., & Niknafs, A., 2014. Nbclust: an r package for  
708 determining the relevant number of clusters in a data set. *J. Stat. Softw.*, *61*, 1–36.
- 709 Chen, T., & Guestrin, C., 2016. Xgboost: A scalable tree boosting system. In *Proceedings of*  
710 *the 22nd ACM sigkdd international conference on knowledge discovery and data mining* (pp.  
711 785–794).

- 712 Chester, D. L., 1990. Why two hidden layers are better than one. In *Proc. IJCNN, Washington,*  
713 *DC* (pp. 265–268). volume 1.
- 714 Chollet, F. et al., 2015. Keras. <https://keras.io>.
- 715 Conson, A. R., Taniguti, C. H., Amadeu, R. R., Andreotti, I. A., de Souza, L. M., dos Santos,  
716 L. H., Rosa, J. R., Mantello, C. C., da Silva, C. C., José Scaloppi Junior, E. et al., 2018.  
717 High-resolution genetic map and qtl analysis of growth-related traits of hevea brasiliensis  
718 cultivated under suboptimal temperature and humidity conditions. *Front. Plant Sci.*, *9*,  
719 1255.
- 720 Cover, T., & Hart, P., 1967. Nearest neighbor pattern classification. *IEEE Trans. Inf. Theory*,  
721 *13*, 21–27.
- 722 Cros, D., Denis, M., Sánchez, L., Cochard, B., Flori, A., Durand-Gasselín, T., Nouy, B., Omoré,  
723 A., Pomiès, V., Riou, V. et al., 2015. Genomic selection prediction accuracy in a perennial  
724 crop: case study of oil palm (*elaeis guineensis jacq.*). *Theor. Appl. Genet.*, *128*, 397–410.
- 725 Cros, D., Mbo-Nkoulou, L., Bell, J. M., Oum, J., Masson, A., Soumahoro, M., Tran, D. M.,  
726 Achour, Z., Le Guen, V., & Clement-Demange, A., 2019. Within-family genomic selection  
727 in rubber tree (*hevea brasiliensis*) increases genetic gain for rubber production. *Ind. Crops*  
728 *Prod.*, *138*, 111464.
- 729 Crossa, J., Jarquín, D., Franco, J., Pérez-Rodríguez, P., Burgueño, J., Saint-Pierre, C., Vikram,  
730 P., Sansaloni, C., Petrolí, C., Akdemir, D. et al., 2016. Genomic prediction of gene bank  
731 wheat landraces. *G3: Genes Genom. Genet.*, *6*, 1819–1834.
- 732 Crossa, J., Martini, J. W., Gianola, D., Pérez-Rodríguez, P., Jarquin, D., Juliana, P.,  
733 Montesinos-López, O., & Cuevas, J., 2019. Deep kernel and deep learning for genome-based  
734 prediction of single traits in multienvironment breeding trials. *Front. Genet.*, *10*.
- 735 Crossa, J., Perez, P., Hickey, J., Burgueno, J., Ornella, L., Cerón-Rojas, J., Zhang, X., Dreisi-  
736 gacker, S., Babu, R., Li, Y. et al., 2014. Genomic prediction in CIMMYT maize and wheat  
737 breeding programs. *Heredity*, *112*, 48–60.

- 738 Crossa, J., Pérez-Rodríguez, P., Cuevas, J., Montesinos-López, O., Jarquín, D., de los Campos,  
739 G., Burgueño, J., González-Camacho, J. M., Pérez-Elizalde, S., Beyene, Y. et al., 2017.  
740 Genomic selection in plant breeding: methods, models, and perspectives. *Trends Plant Sci.*,  
741 *22*, 961–975.
- 742 Cuevas, J., Crossa, J., Soberanis, V., Pérez-Elizalde, S., Pérez-Rodríguez, P., Campos, G. d. l.,  
743 Montesinos-López, O., & Burgueño, J., 2016. Genomic prediction of genotype  $\times$  environment  
744 interaction kernel regression models. *Plant Genome*, *9*.
- 745 Da Silva, I. N., Spatti, D. H., Flauzino, R. A., Liboni, L. H. B., & dos Reis Alves, S. F., 2017.  
746 Artificial Neural Networks. *Cham: Springer International Publishing*, (p. 39).
- 747 Danecek, P., Auton, A., Abecasis, G., Albers, C. A., Banks, E., DePristo, M. A., Handsaker,  
748 R. E., Lunter, G., Marth, G. T., Sherry, S. T. et al., 2011. The variant call format and  
749 VCFtools. *Bioinformatics*, *27*, 2156–2158.
- 750 De Los Campos, G., Naya, H., Gianola, D., Crossa, J., Legarra, A., Manfredi, E., Weigel, K., &  
751 Cotes, J. M., 2009. Predicting quantitative traits with regression models for dense molecular  
752 markers and pedigree. *Genetics*, *182*, 375–385.
- 753 Dijkman, M. J. et al., 1951. Hevea, thirty years of research in the far east. *Hevea, Thirty years*  
754 *of research in the Far East.*
- 755 Elshire, R. J., Glaubitz, J. C., Sun, Q., Poland, J. A., Kawamoto, K., Buckler, E. S., & Mitchell,  
756 S. E., 2011. A robust, simple genotyping-by-sequencing (GBS) approach for high diversity  
757 species. *PLoS One*, *6*.
- 758 Endelman, J. B., 2011. Ridge regression and other kernels for genomic selection with R package  
759 rrBLUP. *Plant Genome*, *4*, 250–255.
- 760 Feng, J., Wang, L., Yu, H., Jiao, L., & Zhang, X., 2019. Divide-and-conquer dual-architecture  
761 convolutional neural network for classification of hyperspectral images. *Remote Sens.*, *11*,  
762 484.

- 763 Francisco, F. R., Aono, A. H., da Silva, C. C., Gonçalves, P. d. S., Scaloppi Junior, E. J.,  
764 Le Guen, V., Neto, R. F., Souza, L. M. D., & de Souza, A. P., 2021. Unravelling rubber tree  
765 growth by integrating GWAS and biological network-based approaches. *Front. Plant Sci.*,  
766 (p. 2719).
- 767 Freund, Y., & Schapire, R. E., 1997. A decision-theoretic generalization of on-line learning and  
768 an application to boosting. *J. Comput. Syst. Sci.*, 55, 119–139.
- 769 Frosyniotis, D., Stafylopatis, A., & Likas, A., 2003. A divide-and-conquer method for multi-net  
770 classifiers. *Pattern Anal. Appl.*, 6, 32–40.
- 771 Fu, W., Breininger, K., Schaffert, R., Ravikumar, N., & Maier, A., 2019. A divide-and-conquer  
772 approach towards understanding deep networks. In *International Conference on Medical*  
773 *Image Computing and Computer-Assisted Intervention* (pp. 183–191). Springer.
- 774 Gianola, D., 2013. Priors in whole-genome regression: The bayesian alphabet returns. *Genetics*,  
775 194, 573–596.
- 776 Gianola, D., Weigel, K. A., Krämer, N., Stella, A., & Schön, C.-C., 2014. Enhancing genome-  
777 enabled prediction by bagging genomic blup. *PLoS One*, 9.
- 778 Glaubitz, J. C., Casstevens, T. M., Lu, F., Harriman, J., Elshire, R. J., Sun, Q., & Buckler,  
779 E. S., 2014. Tassel-GBS: A high capacity genotyping by sequencing analysis pipeline. *PLoS*  
780 *One*, 9, e90346.
- 781 Gonçalves, P. d. S., Rossetti, A. G., Valois, A. C. C., & Viegas, I., 1984. Estimativas de  
782 correlações genéticas e fenotípicas de alguns caracteres quantitativos em clones jovens de  
783 seringueira (hevea spp). *Embrapa Amazônia Ocidental-Artigo em periódico indexado (AL-*  
784 *ICE)*.
- 785 González-Camacho, J., de Los Campos, G., Pérez, P., Gianola, D., Cairns, J., Mahuku, G.,  
786 Babu, R., & Crossa, J., 2012. Genome-enabled prediction of genetic values using radial basis  
787 function neural networks. *Theor. Appl. Genet.*, 125, 759–771.

- 788 González-Camacho, J. M., Ornella, L., Pérez-Rodríguez, P., Gianola, D., Dreisigacker, S., &  
789 Crossa, J. 2018. Applications of machine learning methods to genomic selection in breeding  
790 wheat for rust resistance. *Plant Genome*, 11.
- 791 Goodnight, C. J., 1989. Population differentiation and the correlation among traits at the  
792 population level. *Am. Nat.*, 133, 888–900.
- 793 Goodstein, D. M., Shu, S., Howson, R., Neupane, R., Hayes, R. D., Fazo, J., Mitros, T., Dirks,  
794 W., Hellsten, U., Putnam, N. et al., 2012. Phytozome: a comparative platform for green  
795 plant genomics. *Nucleic Acids Res.*, 40, D1178–D1186.
- 796 Granato, I., Cuevas, J., Luna-Vázquez, F., Crossa, J., Montesinos-López, O., Burgueño, J., &  
797 Fritsche-Neto, R., 2018a. BGGE: a new package for genomic-enabled prediction incorporating  
798 genotype  $\times$  environment interaction models. *G3: Genes Genom. Genet.*, 8, 3039–3047.
- 799 Granato, I. S., Galli, G., de Oliveira Couto, E. G., e Souza, M. B., Mendonça, L. F., & Fritsche-  
800 Neto, R., 2018b. snpready: a tool to assist breeders in genomic analysis. *Mol. Breed.*, 38,  
801 102.
- 802 Grattapaglia, D., 2017. Status and perspectives of genomic selection in forest tree breeding. In  
803 *Genomic Selection for Crop Improvement* (pp. 199–249). Springer, New York.
- 804 Guo, Z., Tucker, D. M., Basten, C. J., Gandhi, H., Ersoz, E., Guo, B., Xu, Z., Wang, D.,  
805 & Gay, G., 2014. The impact of population structure on genomic prediction in stratified  
806 populations. *Theor. Appl. Genet.*, 127, 749–762.
- 807 Harfouche, A. L., Jacobson, D. A., Kainer, D., Romero, J. C., Harfouche, A. H., Mugnozza,  
808 G. S., Moshelion, M., Tuskan, G. A., Keurentjes, J. J., & Altman, A., 2019. Accelerating  
809 climate resilient plant breeding by applying next-generation artificial intelligence. *Trends*  
810 *Biotechnol.*
- 811 Hayes, B., Goddard, M. et al., 2001. Prediction of total genetic value using genome-wide dense  
812 marker maps. *Genetics*, 157, 1819–1829.

- 813 Hayes, B. J., Lewin, H. A., & Goddard, M. E., 2013. The future of livestock breeding: genomic  
814 selection for efficiency, reduced emissions intensity, and adaptation. *Trends Genet.*, *29*, 206–  
815 214.
- 816 Hecht-Nielsen, R., 1987. Kolmogorov’s mapping neural network existence theorem. In *Pro-*  
817 *ceedings of the International Conference on Neural Networks* (pp. 11–14). IEEE Press, New  
818 York volume 3.
- 819 Hecht-Nielsen, R., 1992. Theory of the backpropagation neural network. In *Neural Networks*  
820 *for Perception* (pp. 65–93). Elsevier.
- 821 Heffner, E. L., Lorenz, A. J., Jannink, J.-L., & Sorrells, M. E., 2010. Plant breeding with  
822 genomic selection: gain per unit time and cost. *Crop Sci.*, *50*, 1681–1690.
- 823 Heslot, N., Yang, H.-P., Sorrells, M. E., & Jannink, J.-L., 2012. Genomic selection in plant  
824 breeding: a comparison of models. *Crop Sci.*, *52*, 146–160.
- 825 Hirschhorn, J. N., Lindgren, C. M., Daly, M. J., Kirby, A., Schaffner, S. F., Burt, N. P.,  
826 Altshuler, D., Parker, A., Rioux, J. D., Platko, J. et al., 2001. Genomewide linkage analysis  
827 of stature in multiple populations reveals several regions with evidence of linkage to adult  
828 height. *Am. J. Hum. Genet.*, *69*, 106–116.
- 829 Hoffer, E., Ben-Nun, T., Hubara, I., Giladi, N., Hoefler, T., & Soudry, D., 2019. Augment your  
830 batch: better training with larger batches. arXiv preprint arXiv:1901.09335.
- 831 Hoffer, E., Hubara, I., & Soudry, D., 2017. Train longer, generalize better: closing the gener-  
832 alization gap in large batch training of neural networks. In *Advances in Neural Information*  
833 *Processing Systems* (pp. 1731–1741).
- 834 Hornik, K., 1993. Some new results on neural network approximation. *Neural Netw.*, *6*, 1069–  
835 1072.
- 836 Hornik, K., Stinchcombe, M., White, H. et al., 1989. Multilayer feedforward networks are  
837 universal approximators. *Neural Netw.*, *2*, 359–366.

- 838 Huang, G.-B., 2003. Learning capability and storage capacity of two-hidden-layer feedforward  
839 networks. *IEEE Trans. Neural Netw.*, *14*, 274–281.
- 840 Inácio, Í. S. C. G. F., & Alves, M. F. C., 2019. Increasing accuracy and reducing costs of  
841 genomic prediction by marker selection. *Euphytica*, *215*, 18.
- 842 Intanagonwiwat, C., 1998. The divide-and-conquer neural network: its architecture and train-  
843 ing. In *1998 IEEE International Joint Conference on Neural Networks Proceedings. IEEE  
844 World Congress on Computational Intelligence (Cat. No. 98CH36227)* (pp. 462–467). IEEE  
845 volume 1.
- 846 Islam, M. M., & Murase, K., 2001. A new algorithm to design compact two-hidden-layer  
847 artificial neural networks. *Neural Netw.*, *14*, 1265–1278.
- 848 Jannink, J.-L., Lorenz, A. J., & Iwata, H., 2010. Genomic selection in plant breeding: from  
849 theory to practice. *Brief. Funct. Genom.*, *9*, 166–177.
- 850 Jarquín, D., Lemes da Silva, C., Gaynor, R. C., Poland, J., Fritz, A., Howard, R., Batten-  
851 field, S., & Crossa, J., 2017. Increasing genomic-enabled prediction accuracy by modeling  
852 genotype  $\times$  environment interactions in kansas wheat. *Plant Genome*, *10*.
- 853 Jiang, N., Zhang, Z., Ma, X., & Wang, J., 2008. The lower bound on the number of hidden  
854 neurons in multi-valued multi-threshold neural networks. In *2008 Second International Sym-  
855 posium on Intelligent Information Technology Application* (pp. 103–107). IEEE volume 1.
- 856 Khan, M. A., Tong, F., Wang, W., He, J., Zhao, T., & Gai, J., 2018. Analysis of QTL-  
857 allele system conferring drought tolerance at seedling stage in a nested association mapping  
858 population of soybean [*Glycine max* (L.) Merr.] using a novel GWAS procedure. *Planta*,  
859 *248*, 947–962.
- 860 Kingma, D. P., & Ba, J., 2014. Adam: A method for stochastic optimization. arXiv preprint  
861 arXiv:1412.6980.
- 862 Kolmogorov, A. N., 1957. On the representation of continuous functions of many variables

- 863 by superposition of continuous functions of one variable and addition. In *Doklady Akademii*  
864 *Nauk* (pp. 953–956). Russian Academy of Sciences volume 114.
- 865 Kumar, S., Molloy, C., Muñoz, P., Daetwyler, H., Chagné, D., & Volz, R., 2015. Genome-  
866 enabled estimates of additive and nonadditive genetic variances and prediction of apple phe-  
867 notypes across environments. *G3: Genes Genom. Genet.*, *5*, 2711–2718.
- 868 Kurková, V., 1992. Kolmogorov’s theorem and multilayer neural networks. *Neural Netw.*, *5*,  
869 501–506.
- 870 Kurková, V., & Sanguineti, M., 2013. Can two hidden layers make a difference? In *International*  
871 *Conference on Adaptive and Natural Computing Algorithms* (pp. 30–39). Springer, New York.
- 872 Lau, N.-S., Makita, Y., Kawashima, M., Taylor, T. D., Kondo, S., Othman, A. S., Shu-Chien,  
873 A. C., & Matsui, M., 2016. The rubber tree genome shows expansion of gene family associated  
874 with rubber biosynthesis. *Sci. Rep.*, *6*, 28594.
- 875 Le Guen, V., Doaré, F., Weber, C., & Seguin, M., 2009. Genetic structure of amazonian pop-  
876 ulations of hevea brasiliensis is shaped by hydrographical network and isolation by distance.  
877 *Tree Genet. Genom.*, *5*, 673–683.
- 878 Le Guen, V., Garcia, D., Doaré, F., Mattos, C. R., Condina, V., Couturier, C., Chambon, A.,  
879 Weber, C., Espéout, S., & Seguin, M., 2011. A rubber tree’s durable resistance to microcyclus  
880 ulei is conferred by a qualitative gene and a major quantitative resistance factor. *Tree Genet.*  
881 *Genom.*, *7*, 877–889.
- 882 Le Guen, V., Garcia, D., Mattos, C. R. R., Doaré, F., Lespinasse, D., & Seguin, M., 2007.  
883 Bypassing of a polygenic microcyclus ulei resistance in rubber tree, analyzed by qtl detection.  
884 *New Phytolog.*, *173*, 335–345.
- 885 Lespinasse, D., Grivet, L., Troispoux, V., Rodier-Goud, M., Pinard, F., & Seguin, M., 2000a.  
886 Identification of QTLs involved in the resistance to South American leaf blight (*Microcyclus*  
887 *ulei*) in the rubber tree. *Theor. Appl. Genet.*, *100*, 975–984.

- 888 Lespinasse, D., Rodier-Goud, M., Grivet, L., Leconte, A., Legnaté, H., & Seguin, M., 2000b.  
889 A saturated genetic linkage map of rubber tree (*Hevea* spp.) based on RFLP, AFLP, mi-  
890 crosatellite, and isozyme markers. *Theor. Appl. Genet.*, *100*, 127–138.
- 891 Li, B., Zhang, N., Wang, Y.-G., George, A. W., Reverter, A., & Li, Y., 2018. Genomic  
892 prediction of breeding values using a subset of SNPs identified by three machine learning  
893 methods. *Front. Genet.*, *9*, 237.
- 894 Li, H., & Durbin, R., 2009. Fast and accurate short read alignment with burrows–wheeler  
895 transform. *Bioinformatics*, *25*, 1754–1760.
- 896 Linhart, Y. B., & Grant, M. C., 1996. Evolutionary significance of local genetic differentiation  
897 in plants. *Ann. Rev. Ecol. Syst.*, *27*, 237–277.
- 898 Liu, J., Shi, C., Shi, C.-C., Li, W., Zhang, Q.-J., Zhang, Y., Li, K., Lu, H.-F., Shi, C., Zhu,  
899 S.-T. et al., 2020. The chromosome-based rubber tree genome provides new insights into  
900 spurge genome evolution and rubber biosynthesis. *Mol. Plant*, *13*, 336–350.
- 901 Liu, X., Wang, H., Wang, H., Guo, Z., Xu, X., Liu, J., Wang, S., Li, W.-X., Zou, C., Prasanna,  
902 B. M. et al., 2018. Factors affecting genomic selection revealed by empirical evidence in  
903 maize. *Crop J.*, *6*, 341–352.
- 904 Liu, Y., Wang, D., He, F., Wang, J., Joshi, T., & Xu, D., 2019. Phenotype prediction and  
905 genome-wide association study using deep convolutional neural network of soybean. *Front.*  
906 *Genet.*, *10*, 1091.
- 907 Long, N., Gianola, D., Rosa, G. J., Weigel, K. A., & Avendaño, S., 2007. Machine learning  
908 classification procedure for selecting SNPs in genomic selection: application to early mortality  
909 in broilers. *J. Anim. Breed. Genet.*, *124*, 377–389.
- 910 Luo, Z., Yu, Y., Xiang, J., & Li, F., 2021. Genomic selection using a subset of SNPs identi-  
911 fied by genome-wide association analysis for disease resistance traits in aquaculture species.  
912 *Aquaculture*, *539*, 736620.

- 913 Ma, W., Qiu, Z., Song, J., Li, J., Cheng, Q., Zhai, J., & Ma, C., 2018. A deep convolutional  
914 neural network approach for predicting phenotypes from genotypes. *Planta*, *248*, 1307–1318.
- 915 Mastrangelo, A. M., Marone, D., Laidò, G., De Leonardis, A. M., & De Vita, P., 2012. Alter-  
916 native splicing: enhancing ability to cope with stress via transcriptome plasticity. *Plant Sci.*,  
917 *185*, 40–49.
- 918 de Mendiburu, F., & de Mendiburu, M. F., 2019. Package ‘agricolae’. *R Package Version*, (pp.  
919 1–2).
- 920 Merilä, J., & Crnokrak, P., 2001. Comparison of genetic differentiation at marker loci and  
921 quantitative traits. *J. Evol. Biol.*, *14*, 892–903.
- 922 Mohamad, M., 2013. Divide and conquer approach in reducing ANN training time for small  
923 and large data. *J. Appl. Sci.*, *13*, 133–139.
- 924 Montesinos-López, O. A., Martín-Vallejo, J., Crossa, J., Gianola, D., Hernández-Suárez, C. M.,  
925 Montesinos-López, A., Juliana, P., & Singh, R., 2019a. A benchmarking between deep  
926 learning, support vector machine and bayesian threshold best linear unbiased prediction for  
927 predicting ordinal traits in plant breeding. *G3: Genes Genom. Genet.*, *9*, 601–618.
- 928 Montesinos-López, O. A., Montesinos-López, A., Crossa, J., Gianola, D., Hernández-Suárez,  
929 C. M., & Martín-Vallejo, J., 2018. Multi-trait, multi-environment deep learning modeling for  
930 genomic-enabled prediction of plant traits. *G3: Genes Genom. Genet.*, *8*, 3829–3840.
- 931 Montesinos-López, O. A., Montesinos-López, A., Tuberosa, R., Maccaferri, M., Sciara, G.,  
932 Ammar, K., & Crossa, J., 2019b. Multi-trait, multi-environment genomic prediction of  
933 durum wheat with genomic best linear unbiased predictor and deep learning methods. *Front.*  
934 *Plant Sci.*, *10*.
- 935 Muñoz, F., & Sanchez, L., 2019. *breedR: Statistical Methods for Forest Genetic Resources*  
936 *Analysts*. URL: <https://github.com/famuvie/breedR> R Package Version 0.12-4.
- 937 Muranty, H., Troggio, M., Sadok, I. B., Al Rifaï, M., Auwerkerken, A., Banchi, E., Velasco, R.,

- 938 Stevanato, P., Van De Weg, W. E., Di Guardo, M. et al., 2015. Accuracy and responses of  
939 genomic selection on key traits in apple breeding. *Hortic. Res.*, *2*, 1–12.
- 940 Murphy, T. M., 2005. What is base excision repair good for? Knockout mutants for FPG and  
941 OGG glycosylase genes in Arabidopsis. *Physiol. Plant.*, *123*, 227–232.
- 942 Nadeem, M. A., Nawaz, M. A., Shahid, M. Q., Doğan, Y., Comertpay, G., Yıldız, M., Hatipoğlu,  
943 R., Ahmad, F., Alsaleh, A., Labhane, N. et al., 2018. Dna molecular markers in plant  
944 breeding: current status and recent advancements in genomic selection and genome editing.  
945 *Biotechnol. Biotechnol. Equip.*, *32*, 261–285.
- 946 Nakkanong, K., Nualsri, C., & Sdoodee, S., 2008. Analysis of genetic diversity in early in-  
947 troduced clones of rubber tree (*hevea brasiliensis*) using rapd and microsatellite markers.  
948 *Songklanakarın J. Sci. Technol.*, *30*.
- 949 O’Connor, K., Hayes, B., & Topp, B., 2018. Prospects for increasing yield in macadamia using  
950 component traits and genomics. *Tree Genet. Genom.*, *14*, 7.
- 951 Ogut, F., Bian, Y., Bradbury, P. J., & Holland, J. B., 2015. Joint-multiple family linkage  
952 analysis predicts within-family variation better than single-family analysis of the maize nested  
953 association mapping population. *Heredity*, *114*, 552–563.
- 954 O’Shea, K., & Nash, R., 2015. An introduction to convolutional neural networks. arXiv preprint  
955 arXiv:1511.08458.
- 956 Pedregosa, F., Varoquaux, G., Gramfort, A., Michel, V., Thirion, B., Grisel, O., Blondel, M.,  
957 Prettenhofer, P., Weiss, R., Dubourg, V. et al., 2011. Scikit-learn: Machine learning in  
958 python. *J. Mach. Learn. Res.*, *12*, 2825–2830.
- 959 Pérez, P., & de Los Campos, G., 2014. Genome-wide regression and prediction with the BGLR  
960 statistical package. *Genetics*, *198*, 483–495.
- 961 Pérez-Rodríguez, P., Gianola, D., González-Camacho, J. M., Crossa, J., Manès, Y., & Dreisi-  
962 gacker, S., 2012. Comparison between linear and non-parametric regression models for  
963 genome-enabled prediction in wheat. *G3: Genes Genom. Genet.*, *2*, 1595–1605.

- 964 Peterson, R., 2017. Estimating normalization transformations with bestnormalize. URL <https://github.com/CompetersonRbestNormalize>.
- 965
- 966 Pimenta, R. J. G., Aono, A. H., Burbano, R. C. V., Coutinho, A. E., da Silva, C. C., Dos Anjos,  
967 I. A., Perecin, D., Landell, M. G. d. A., Gonçalves, M. C., Pinto, L. R. et al., 2021. Genome-  
968 wide approaches for the identification of markers and genes associated with sugarcane yellow  
969 leaf virus resistance. *Sci. Rep.*, *11*, 1–18.
- 970 Popescu, M.-C., Balas, V. E., Perescu-Popescu, L., & Mastorakis, N., 2009. Multilayer percep-  
971 tron and neural networks. *WSEAS Transactions on Circuits and Systems*, *8*, 579–588.
- 972 Pressoir, G., & Berthaud, J., 2004. Patterns of population structure in maize landraces from  
973 the central valleys of Oaxaca in Mexico. *Heredity*, *92*, 88–94.
- 974 Ramzan, F., Gültas, M., Bertram, H., Cavero, D., & Schmitt, A. O., 2020. Combining random  
975 forests and a signal detection method leads to the robust detection of genotype-phenotype  
976 associations. *Genes*, *11*, 892.
- 977 Rao, G. P., & Kole, P., 2016. Evaluation of brazilian wild hevea germplasm for cold tolerance:  
978 genetic variability in the early mature growth. *J. For. Res.*, *27*, 755–765.
- 979 Raymond, B., Bouwman, A. C., Schrooten, C., Houwing-Duistermaat, J., & Veerkamp, R. F.,  
980 2018. Utility of whole-genome sequence data for across-breed genomic prediction. *Genet.*  
981 *Sel. Evol.*, *50*, 1–12.
- 982 Roldán-Arjona, T., Ariza, R. R., & Córdoba-Cañero, D., 2019. Dna base excision repair in  
983 plants: An unfolding story with familiar and novel characters. *Front. Plant Sci.*, *10*, 1055.
- 984 Romain, B., & Thierry, C., 2011. Rubberclones (hevea clonal descriptions).
- 985 Roorkiwal, M., Jarquin, D., Singh, M. K., Gaur, P. M., Bharadwaj, C., Rathore, A., Howard,  
986 R., Srinivasan, S., Jain, A., Garg, V. et al., 2018. Genomic-enabled prediction models using  
987 multi-environment trials to estimate the effect of genotype× environment interaction on  
988 prediction accuracy in chickpea. *Sci. Rep.*, *8*, 1–11.

- 989 Roorkiwal, M., Rathore, A., Das, R. R., Singh, M. K., Jain, A., Srinivasan, S., Gaur, P. M.,  
990 Chellapilla, B., Tripathi, S., Li, Y. et al., 2016. Genome-enabled prediction models for yield  
991 related traits in chickpea. *Front. Plant Sci.*, 7, 1666.
- 992 Rosa, J. R. B. F., Mantello, C. C., Garcia, D., de Souza, L. M., Da Silva, C. C., Gazaffi, R.,  
993 da Silva, C. C., Toledo-Silva, G., Cubry, P., Garcia, A. A. F. et al., 2018. QTL detection for  
994 growth and latex production in a full-sib rubber tree population cultivated under suboptimal  
995 climate conditions. *BMC Plant Biol.*, 18, 223.
- 996 Rumelhart, D. E., 1986. Learning representations by error propagation, in de rumelhart, jl  
997 mcclelland & pdp research group. *Parallel Distrib. Proc.*, 1.
- 998 Sakhakarmi, S., & Park, J. W., 2020. Multi-level-phase deep learning using divide-and-conquer  
999 for scaffolding safety. *Int. J. Environ. Res. Public Health*, 17, 2391.
- 1000 Shawe-Taylor, J., & Cristianini, N., 2000. *An introduction to support vector machines and other*  
1001 *kernel-based learning methods* volume 204.
- 1002 Sheela, K. G., & Deepa, S. N., 2013. Review on methods to fix number of hidden neurons in  
1003 neural networks. *Math. Probl. Eng.*, 2013.
- 1004 Sivakumaran, S., Haridas, G., & Abraham, P., 1988. Problem of tree dryness with high yielding  
1005 precocious clones and methods to exploit such clones. *Proc. Coll. Hevea*, 88, 253–267.
- 1006 Smith, D. R., 1985. The design of divide and conquer algorithms. *Sci. Comput. Program.*, 5,  
1007 37–58.
- 1008 Sontag, E. D., 1991. Feedback stabilization using two-hidden-layer nets. In *1991 American*  
1009 *Control Conference* (pp. 815–820). IEEE.
- 1010 Souza, L. M., Gazaffi, R., Mantello, C. C., Silva, C. C., Garcia, D., Le Guen, V., Cardoso, S.  
1011 E. A., Garcia, A. A. F., & Souza, A. P., 2013. Qtl mapping of growth-related traits in a  
1012 full-sib family of rubber tree (*hevea brasiliensis*) evaluated in a sub-tropical climate. *PLoS*  
1013 *One*, 8.

- 1014 de Souza, L. M., Toledo-Silva, G., Cardoso-Silva, C. B., Da Silva, C. C., de Araujo Andreotti,  
1015 I. A., Conson, A. R. O., Mantello, C. C., Le Guen, V., & de Souza, A. P., 2016. Development  
1016 of single nucleotide polymorphism markers in the large and complex rubber tree genome  
1017 using next-generation sequence data. *Mol. Breed.*, *36*, 115.
- 1018 Souza, L. M. d., Francisco, F. R., Gonçalves, P. d. S., Scaloppi-Junior, E. J. J., Le Guen, V.,  
1019 Fritsche-Neto, R., & Souza, A. P. d., 2019. Genomic selection in rubber tree breeding: A  
1020 comparison of models and methods for managing  $g \times e$  interactions. *Front. Plant Sci.*, *10*,  
1021 1353.
- 1022 Spindel, J., Begum, H., Akdemir, D., Virk, P., Collard, B., Redona, E., Atlin, G., Jannink,  
1023 J.-L., & McCouch, S. R., 2015. Genomic selection and association mapping in rice (*Oryza*  
1024 *sativa*): effect of trait genetic architecture, training population composition, marker number  
1025 and statistical model on accuracy of rice genomic selection in elite, tropical rice breeding  
1026 lines. *PLoS Genet.*, *11*, e1004982.
- 1027 Stathakis, D., 2009. How many hidden layers and nodes? *Int. J. Remote Sens.*, *30*, 2133–2147.
- 1028 Stewart-Brown, B. B., Song, Q., Vaughn, J. N., & Li, Z., 2019. Genomic selection for yield and  
1029 seed composition traits within an applied soybean breeding program. *G3: Genes Genom.*  
1030 *Genet.*, *9*, 2253–2265.
- 1031 Szakonyi, D., & Duque, P., 2018. Alternative splicing as a regulator of early plant development.  
1032 *Front. Plant Sci.*, *9*, 1174.
- 1033 Tang, C., Yang, M., Fang, Y., Luo, Y., Gao, S., Xiao, X., An, Z., Zhou, B., Zhang, B., Tan, X.  
1034 et al., 2016. The rubber tree genome reveals new insights into rubber production and species  
1035 adaptation. *Nat. Plants*, *2*, 1–10.
- 1036 Team, R. C. et al., 2013. R: A language and environment for statistical computing.
- 1037 Thomas, A. J., Petridis, M., Walters, S. D., Gheytaoui, S. M., & Morgan, R. E., 2017. Two  
1038 hidden layers are usually better than one. In *International Conference on Engineering Ap-*  
1039 *plications of Neural Networks* (pp. 279–290). Springer, New York.

- 1040 Tran, D. M., Clément-Demange, A., Deon, M., Garcia, D., Le Guen, V., Clément-Vidal, A.,  
1041 Soumahoro, M., Masson, A., Label, P., Le, M. T. et al., 2016. Genetic determinism of  
1042 sensitivity to corynespora cassiicola exudates in rubber tree (*hevea brasiliensis*). *PLoS One*,  
1043 *11*.
- 1044 VanRaden, P., 2007. Genomic measures of relationship and inbreeding. *INTERBULL bulletin*,  
1045 (pp. 33–33).
- 1046 VanRaden, P. M., 2008. Efficient methods to compute genomic predictions. *J. Dairy Sci.*, *91*,  
1047 4414–4423.
- 1048 Varshney, R. K., 2016. Exciting journey of 10 years from genomes to fields and markets: some  
1049 success stories of genomics-assisted breeding in chickpea, pigeonpea and groundnut. *Plant*  
1050 *Sci.*, *242*, 98–107.
- 1051 Venkatachalam, P., Priya, P., Gireesh, T., Amma, C. S., & Thulaseedharan, A., 2006. Molecular  
1052 cloning and sequencing of a polymorphic band from rubber tree [*hevea brasiliensis* (muell.)  
1053 arg.]: the nucleotide sequence revealed partial homology with proline-specific permease gene  
1054 sequence. *Current Sci.*, (pp. 1510–1515).
- 1055 Waldmann, P., Pfeiffer, C., & Mészáros, G., 2020. Sparse convolutional neural networks for  
1056 genome-wide prediction. *Front. Genet.*, *11*.
- 1057 Wang, Q., Yu, Y., Yuan, J., Zhang, X., Huang, H., Li, F., & Xiang, J., 2017. Effects of marker  
1058 density and population structure on the genomic prediction accuracy for growth trait in  
1059 pacific white shrimp *litopenaeus vannamei*. *BMC Genet.*, *18*, 1–9.
- 1060 Wang, S.-C., 2003. Artificial neural network. In *Interdisciplinary Computing in Java Program-*  
1061 *ming* (pp. 81–100). Springer, New York.
- 1062 Wang, X., Xu, Y., Hu, Z., & Xu, C., 2018. Genomic selection methods for crop improvement:  
1063 Current status and prospects. *Crop J.*, *6*, 330–340.
- 1064 Warren-Thomas, E., Dolman, P. M., & Edwards, D. P., 2015. Increasing demand for natural

- 1065 rubber necessitates a robust sustainability initiative to mitigate impacts on tropical biodi-  
1066 versity. *Conserv. Lett.*, *8*, 230–241.
- 1067 Washburn, J. D., Burch, M. B., Franco, V., & José, A., 2019. Predictive breeding for maize:  
1068 Making use of molecular phenotypes, machine learning, and physiological crop models. *Crop*  
1069 *Sci.*
- 1070 Wei, H., Lou, Q., Xu, K., Yan, M., Xia, H., Ma, X., Yu, X., & Luo, L., 2017. Alternative splicing  
1071 complexity contributes to genetic improvement of drought resistance in the rice maintainer  
1072 huhan2b. *Sci. Rep.*, *7*, 1–13.
- 1073 Wickham, H., 2016. *ggplot2: elegant graphics for data analysis*. Springer, New York.
- 1074 Wolfe, M. D., Del Carpio, D. P., Alabi, O., Ezenwaka, L. C., Ikeogu, U. N., Kayondo, I. S.,  
1075 Lozano, R., Okeke, U. G., Ozimati, A. A., Williams, E. et al., 2017. Prospects for genomic  
1076 selection in cassava breeding. *Plant Genome*, *10*.
- 1077 Würschum, T., 2012. Mapping QTL for agronomic traits in breeding populations. *Theor. Appl.*  
1078 *Genet.*, *125*, 201–210.
- 1079 Xavier, A., Muir, W. M., & Rainey, K. M., 2016. Assessing predictive properties of genome-wide  
1080 selection in soybeans. *G3: Genes Genom. Genet.*, *6*, 2611–2616.
- 1081 Yin, B., Balvert, M., van der Spek, R. A., Dutilh, B. E., Bohte, S., Veldink, J., & Schönhuth,  
1082 A., 2019. Using the structure of genome data in the design of deep neural networks for  
1083 predicting anyotrophic lateral sclerosis from genotype. *Bioinformatics*, *35*, i538–i547.
- 1084 Yu, G., Smith, D. K., Zhu, H., Guan, Y., & Lam, T. T.-Y., 2017. ggtree: an r package for  
1085 visualization and annotation of phylogenetic trees with their covariates and other associated  
1086 data. *Methods Ecol. Evol.*, *8*, 28–36.
- 1087 Zhang, A., Wang, H., Beyene, Y., Semagn, K., Liu, Y., Cao, S., Cui, Z., Ruan, Y., Burgueño,  
1088 J., San Vicente, F. et al., 2017. Effect of trait heritability, training population size and  
1089 marker density on genomic prediction accuracy estimation in 22 bi-parental tropical maize  
1090 populations. *Front. Plant Sci.*, *8*, 1916.

1091 Zhang, C., Stratopoulos, L. M. F., Pretzsch, H., & Rötzer, T., 2019. How do tilia cordata  
1092 greenspire trees cope with drought stress regarding their biomass allocation and ecosystem  
1093 services? *Forests*, *10*, 676.

1094 Zhao, Y., Gowda, M., Liu, W., Würschum, T., Maurer, H. P., Longin, F. H., Ranc, N., & Reif,  
1095 J. C., 2012. Accuracy of genomic selection in european maize elite breeding populations.  
1096 *Theor. Appl. Genet.*, *124*, 769–776.

1097 Zingaretti, L. M., Gezan, S. A., Ferrão, L. F. V., Osorio, L. F., Monfort, A., Muñoz, P. R.,  
1098 Whitaker, V. M., & Pérez-Enciso, M., 2020. Exploring deep learning for complex trait  
1099 genomic prediction in polyploid outcrossing species. *Front. Plant Sci.*, *11*, 25.